Construction and Building Materials 126 (2016) 641–660

Contents lists available at ScienceDirect

Construction and Building Materials

journal homepage: www.elsevier.com/locate/conbuildmat

Review

# Recycling and reuse of construction and demolition waste in concrete-filled steel tubes: A review

Zongping Chen [a,d], Jinjun Xu [b,*], Yuliang Chen [a], Eric M. Lui [c]

[a] College of Civil Engineering and Architecture, Guangxi University, 530004 Nanning, China
[b] College of Civil Engineering, Nanjing Technology University, 211816 Nanjing, China
[c] Department of Civil and Environmental Engineering, Syracuse University, NY 13244-1240, Syracuse, USA
[d] Key Laboratory of Disaster Prevention and Structural Safety of Ministry of Education, Guangxi University, 530004 Nanning, China

## HIGHLIGHTS

- Bond behavior between recycled aggregate concrete and steel tubes was reviewed and discussed.
- Static behavior and long-term performance of RACFT members were summarized.
- Performance of recycled aggregate concrete-filled steel tube members and frames under cyclic loads were described.
- Strength prediction model of recycled aggregate concrete-filled steel tubes was proposed.

## ARTICLE INFO

*Article history:*
Received 23 April 2016
Received in revised form 8 August 2016
Accepted 17 September 2016

*Keywords:*
Recycled coarse aggregate (RCA)
Natural aggregate concrete (NAC)
Recycled aggregate concrete (RAC)
Concrete-filled steel tubes
Bond behavior
Cyclic performance

## ABSTRACT

This paper presents a summary review of research performed on the mechanical behavior of concrete-filled steel tube members and frames made from recycled aggregate concrete (RAC). The paper begins with an introduction of some research progress made on the bond behavior between RAC and steel tubes. Discussion is then turned to the static behavior of recycled aggregate concrete-filled steel tube (RACFST) members, including the flexural performance of beams, concentric and eccentric load carrying capacities of stub columns and long-term performance of columns. Research findings on the performance of RACFST columns and RACFST plane frame under cyclic loads are then presented. The paper concludes with a presentation of a prediction model for the strength of RACFST by considering whether the recycled coarse aggregates have been pre-wetted or not before fabrication of the structural members. Based on these research results, it can be concluded that with proper design and construction, the application of RAC as a structural material in concrete-filled steel tube structures is feasible and safe.



**Contents**



* Corresponding author.
*E-mail address:* jjxu_concrete@163.com (J. Xu).

http://dx.doi.org/10.1016/j.conbuildmat.2016.09.063
0950-0618/

## 1. Introduction

The construction industry is an important economic sector that has a large environmental impact in terms of natural resources extraction, energy consumption, pollutants release, greenhouse gases emissions and amount of waste generated [1]. Hence, promoting and practicing sustainability in construction can help preserve the planet's ecosystems, conserve natural resources and improve the environmental conditions of all living organisms on earth. Recycling and reuse of construction and demolition wastes is one such attempt to achieve this goal. Processing construction and demolition wastes and reintroducing them as recycled aggregates in new concrete, referred to as recycled aggregate concrete (RAC), can be an effective way to develop and implement "green" concrete for new construction.

A review of existing literature [2–9] has shown that much effort has been devoted to the investigation of the mechanical properties and durability of RAC. Thereupon, a basic consensus is that the compressive and tensile strengths, elastic modulus and durability of RAC are in general lower than those of natural aggregate concrete (NAC), but the strain that corresponds to the peak stress, shrinkage and creep of RAC are to a certain extent higher when compared with NAC. Many investigators have demonstrated that the existence of residual mortar lumps adhering to the recycled aggregates as well as the formation of micro-cracks during the crushing process in recycled aggregate production can reduce strength and increase deformation in RAC materials. Regardless of the technical level, the labor costs and additional energy consumption may be enlarged when crushing the construction and demolition waste and producing the recycled aggregates. In addition, common people are lack of confidence on RAC. Therefore, the development and applications of RAC in structures are somewhat restricted due to the above-mentioned shortcomings.

Confining concrete in steel tubes has long been recognized as an effective means to improve the behavior of concrete not only because confinement increases the compressive strength of concrete and helps suppress crack development, but the core concrete is sealed from moisture exchange with the surroundings and its lateral deformation is significantly restricted by the steel tubes [10,11]. Konno et al. [12] were the first to put forth the idea of placing recycled aggregate concrete in steel tubes, with the aim toward improving the mechanical properties of RAC. The resulting structural member is called recycled aggregate concrete-filled steel tube (RACFST). Since then, other researchers have conducted studies to evaluate the effective use of construction and demolition wastes as recycled aggregates in various types of steel tubes, including carbon steel tubes, stainless steel tubes and carbon steel tubes strengthened with fiber reinforced polymers.

In fact, the greatest distinctive feature of RCAs compared to NCAs is their higher water absorption capacity, due mainly to adhered mortar [13,14]. In other words, the additional absorbing moisture of RCA can reduce the actual water-cement ratio ($w/c$) in concrete when RCAs are not pre-wetted, which means that there is a curing effect on the concrete strength. This finding has been confirmed by Chen et al. [15]. However, many researchers launched the investigations on mechanical properties of RAC by the way of pre-wetting the RCAs, so that the workability of RAC can be improved during the construction process [16–18]. Hence, it is not difficult to understand that the strength of RACFST can be varied depending on whether the RCA are presoaked or not.

The primary objective of this paper is to summarize some important findings on the behavior of RACFST when used as isolated flexural and compression members and as members of a frame. A secondary objective is to provide a knowledge basis for further studies on the use of recycled concrete in structural and construction applications.

## 2. Bond behavior between RAC and steel tubes

One of the most important requirements for concrete-filled steel tube (CFST) construction is the integrity of the bond between concrete and steel. Using pushout tests as shown in Fig. 1, Chen et al. [19] studied the bond behavior between the core RAC and the outer steel tubes without surface preparation. The main information about the specimens is given in Table 1 and the results are shown in Fig. 2.

It can be seen from Fig. 2 that the bond strength in general increased with an increase in RCA replacement percentage, except for cases when the recycled aggregate concrete-filled circular steel tubes have replacement percentages of $r = 75\%$ and 100%. It is worth noting that in the study of Ref. [13], the recycled coarse aggregates used in manufacturing RACFST were not pre-soaked,

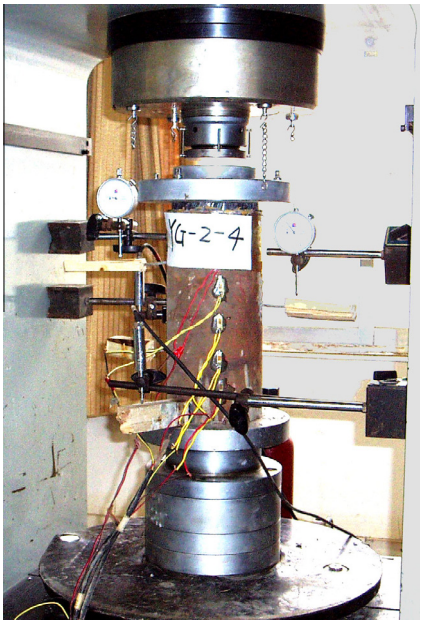


**Fig. 1.** Push-out test set-up (Chen et al. [19]).

**Table 1**
Push-out test specimens.

| Specimen | Section | $D$ (or $B$) × $t$ (mm) [a] | $r$ (%) [a] | Concrete type | $f_{cu}$ (MPa) [a] | $f_y$ (MPa) [a] | $L_e$ (mm) [a] |
|---|---|---|---|---|---|---|---|
| S-RAC-12 | Circular | 140 × 3 | 0 | C50 | 58.5 | 345.90 | 410 |
| S-RAC-13 | | 140 × 3 | 25 | C50 | 59.2 | 345.90 | 410 |
| S-RAC-14 | | 140 × 3 | 50 | C50 | 57.6 | 345.90 | 410 |
| S-RAC-15 | | 140 × 3 | 75 | C50 | 56.8 | 345.90 | 410 |
| S-RAC-16 | | 140 × 3 | 100 | C50 | 55.5 | 345.90 | 410 |
| S-RAC-17 | | 140 × 3 | 0 | C50 | 58.5 | 345.90 | 260 |
| S-RAC-18 | | 140 × 3 | 25 | C50 | 59.2 | 345.90 | 260 |
| S-RAC-19 | | 140 × 3 | 50 | C50 | 57.6 | 345.90 | 260 |
| S-RAC-20 | | 140 × 3 | 75 | C50 | 56.8 | 345.90 | 260 |
| S-RAC-21 | | 140 × 3 | 100 | C50 | 55.5 | 345.90 | 260 |
| S-RAC-22 | Square | 120 × 3 | 25 | C50 | 59.2 | 303.27 | 410 |
| S-RAC-23 | | 120 × 3 | 50 | C50 | 57.6 | 303.27 | 410 |
| S-RAC-24 | | 120 × 3 | 75 | C50 | 56.8 | 303.27 | 410 |
| S-RAC-25 | | 120 × 3 | 100 | C50 | 55.5 | 303.27 | 410 |
| S-RAC-26 | | 120 × 3 | 0 | C50 | 58.5 | 303.27 | 260 |
| S-RAC-27 | | 120 × 3 | 25 | C50 | 59.2 | 303.27 | 260 |
| S-RAC-28 | | 120 × 3 | 50 | C50 | 57.6 | 303.27 | 260 |
| S-RAC-29 | | 120 × 3 | 75 | C50 | 56.8 | 303.27 | 260 |
| S-RAC-30 | | 120 × 3 | 100 | C50 | 55.5 | 303.27 | 260 |
| S-RAC-31 | | 120 × 3 | 75 | C30 | 40.5 | 303.27 | 260 |

[a] $D$ (or $B$) and $t$ are the outside diameter (or width) and wall thickness of the steel tube; $r$ is the RCA replacement percentage; $f_{cu}$ is the compressive concrete cube ($150 \times 150 \times 150$ mm$^3$) strength measured at the time of testing; $f_y$ is the steel tube yield strength; $L_e$ is the embedment length between concrete and steel tube.

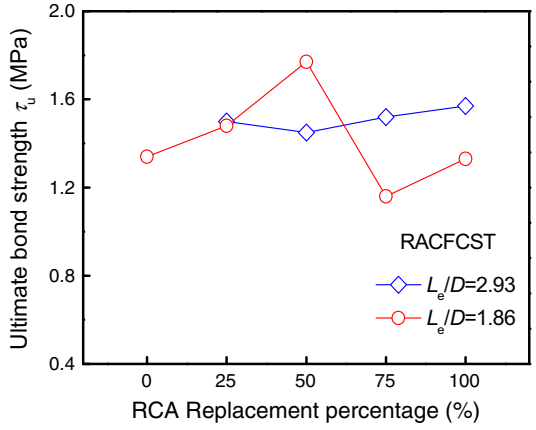


(a) Recycled aggregate concrete-filled circular steel tubes (RACFCST)

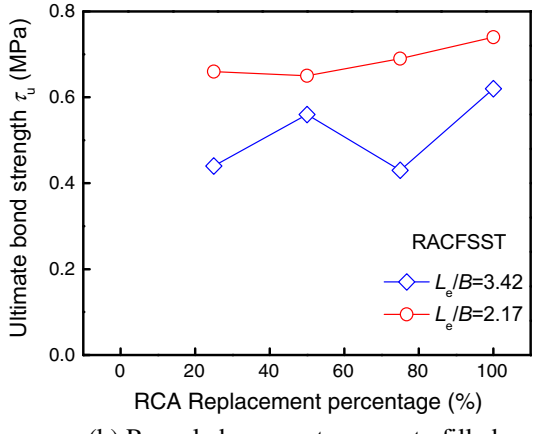


(b) Recycled aggregate concrete-filled square steel tubes (RACFSST)

**Fig. 2.** Effect of RCA content on ultimate bond strength (Chen et al. [19]).

and the design water-cement ratios ($w/c$) were kept constant for all the specimens. Compared to the design $w/c$, the actual $w/c$ in recycled aggregate concrete is lower due to the high water absorption

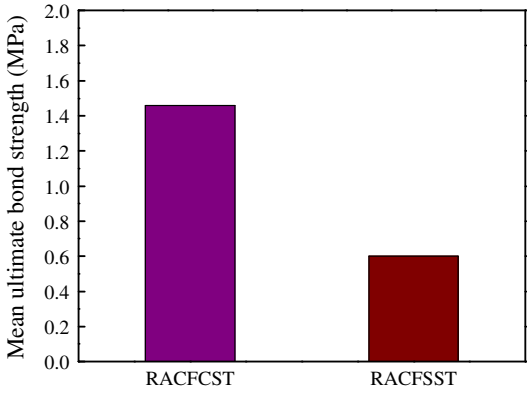


**Fig. 3.** Effect of tube type on ultimate bond strength (Chen et al. [19]).

rate of RCA. This means that the strength of RAC can be enhanced with an increase of RCA content. Butler et al. [20] has demonstrated that higher concrete strength is the result of larger bond strength between RAC and the reinforcement. In addition, Chen et al. [19] have investigated the differences in bond strength between recycled aggregate concrete placed in circular steel tubes and recycled aggregate concrete placed in square steel tubes. It can be seen from Fig. 3 that the bond strength between RAC and circular steel tubes is significantly higher than that between RAC and square steel tubes, indicating that the confinement offered by circular steel tubes is more efficient when compared to square steel tubes under the same parametric conditions. This finding is similar to that for conventional concrete-filled steel tubes [21].

## 3. Performance of RACFST under static loads

### 3.1. Flexural behavior of RACFST beams

Yang and Han [22] reported that RCA replacement percentage (0%, 25% and 50%) did not have much impact on the failure modes of RACFST beams tested under flexural loads as all the test specimens failed by local buckling of the steel tubes in the compression zone. Table 2 gives details of the test specimens and the test results. Fig. 4 shows the test specimens after failure.

**Table 2**
Beam specimens and test results.

| Specimen | Section | $f_{cu}$ (MPa) | $r$ (%) | Tube type | $D$ (or $B$) × $t$ × $L$ (mm) [a] | $f_y$ (MPa) | $M_{ue}$ (kN·m) [a] | SI [a] |
|---|---|---|---|---|---|---|---|---|
| Yang and Han [22] | | | | | | | | |
| BSb0 | Square | 42.7 | 0 | Carbon steel | 150 × 2.94 × 1200 | 344.4 | 34.9 | 0 |
| BSb1 | Square | 41.8 | 25 | Carbon steel | 150 × 2.94 × 1200 | 344.4 | 33.8 | 3.15 |
| BSb2 | Square | 36.6 | 50 | Carbon steel | 150 × 2.94 × 1200 | 344.4 | 33.0 | 5.44 |
| BCb0 | Circular | 42.7 | 0 | Carbon steel | 165 × 2.57 × 1200 | 343.1 | 29.4 | 0 |
| BCb1 | Circular | 41.8 | 25 | Carbon steel | 165 × 2.57 × 1200 | 343.1 | 28.15 | 4.25 |
| BCb2 | Circular | 36.6 | 50 | Carbon steel | 165 × 2.57 × 1200 | 343.1 | 27.65 | 5.95 |
| Yang and Ma [23] | | | | | | | | |
| S-B-N | Square | 63.4 | 0 | Stainless steel | 120 × 1.77 × 1200 | 286.7 | 15.2 | 0 |
| S-B-C1 | Square | 59.7 | 25 | Stainless steel | 120 × 1.77 × 1200 | 286.7 | 14.7 | 3.81 |
| S-B-C2 | Square | 57.3 | 50 | Stainless steel | 120 × 1.77 × 1200 | 286.7 | 14.3 | 6.04 |
| S-B-C3 | Square | 56.9 | 75 | Stainless steel | 120 × 1.77 × 1200 | 286.7 | 14.4 | 5.71 |
| S-B-F1 | Square | 58.6 | 25 | Stainless steel | 120 × 1.77 × 1200 | 286.7 | 14.6 | 4.46 |
| S-B-F2 | Square | 56.2 | 50 | Stainless steel | 120 × 1.77 × 1200 | 286.7 | 14.3 | 6.43 |
| S-B-F3 | Square | 55.3 | 75 | Stainless steel | 120 × 1.77 × 1200 | 286.7 | 13.6 | 10.51 |
| C-B-N | Circular | 63.4 | 0 | Stainless steel | 120 × 1.77 × 1200 | 286.7 | 11.7 | 0 |
| C-B-C1 | Circular | 59.7 | 25 | Stainless steel | 120 × 1.77 × 1200 | 286.7 | 11.6 | 1.28 |
| C-B-C2 | Circular | 57.3 | 50 | Stainless steel | 120 × 1.77 × 1200 | 286.7 | 11.6 | 1.37 |
| C-B-C3 | Circular | 56.9 | 75 | Stainless steel | 120 × 1.77 × 1200 | 286.7 | 11.5 | 1.54 |
| C-B-F1 | Circular | 58.6 | 25 | Stainless steel | 120 × 1.77 × 1200 | 286.7 | 11.5 | 1.79 |
| C-B-F2 | Circular | 56.2 | 50 | Stainless steel | 120 × 1.77 × 1200 | 286.7 | 10.6 | 9.30 |
| C-B-F3 | Circular | 55.3 | 75 | Stainless steel | 120 × 1.77 × 1200 | 286.7 | 10.6 | 9.56 |

[a] $L$ is the specimen length; $M_{ue}$ is the experimentally obtained ultimate moment, SI is the strength index expressed in Eq. (12).

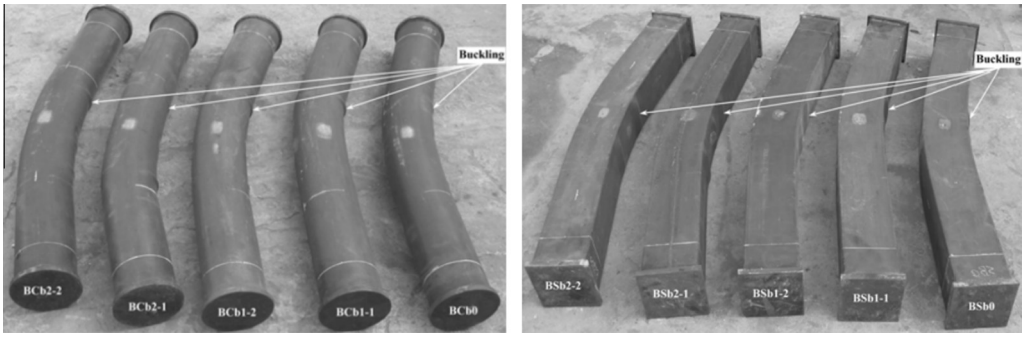


**Fig. 4.** Failure modes of RAC-filled carbon steel tube beams (Yang and Han [22]).

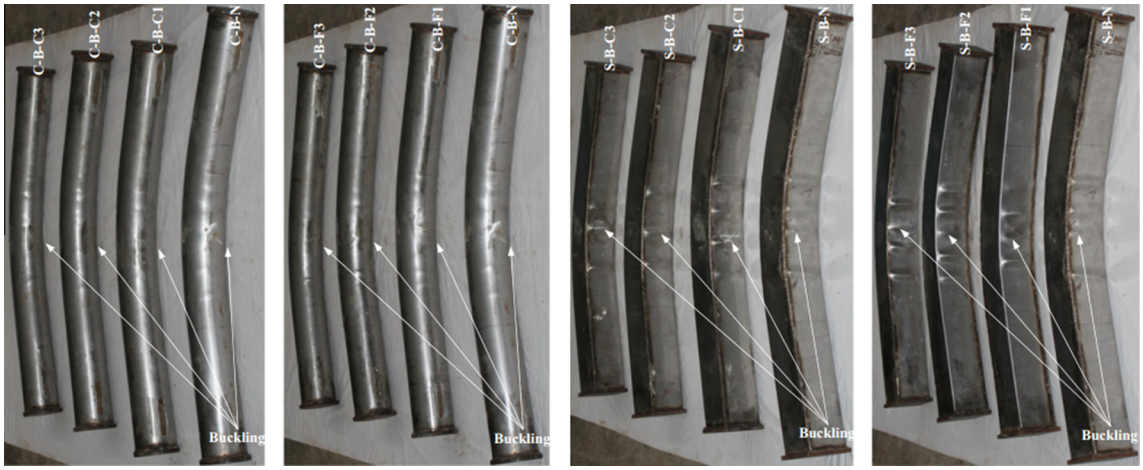


**Fig. 5.** Failure modes of RAC-filled stainless steel tube beams (Yang and Ma [23]).

From Fig. 4, it can be seen that local buckling failure was distributed more or less equally and symmetrically about midspan of the specimens. However, the initial section flexural stiffness and serviceability-level section flexural stiffness of the beams with RAC were found to be 3.3–8.7%, and 3.1–8.2% lower than those of the beams with conventional concrete, respectively; and the ultimate bending moment of the specimens with conventional concrete were 3.5–8.1% more resistant than that of beams with RAC.

For use in marine environments where corrosion is severe, stainless steel tubes can be used in place of carbon steel tubes as

**Table 3**
Concentrically loaded column specimens.

| Specimen | Section | $f_{cu}$ (MPa) | $r$ (%) | Tube type | $D$ (or $B$) × $t$ × $L$ (mm) [a] | $f_y$ (MPa) | $N_{ue}$ (kN) [a] | fcc/fc | Ess/Ec | SI [a] |
|---|---|---|---|---|---|---|---|---|---|---|
| Yang and Han [22] | | | | | | | | | | |
| Ca0 | Circular | 42.7 | 0 | Carbon steel | 114 × 2.19 × 342 | 335.7 | 741.0 | 2.13 | 1.14 | 0 |
| Ca1 | Circular | 41.8 | 25 | Carbon steel | 114 × 2.19 × 342 | 335.7 | 705.5 | 2.07 | 1.18 | 4.79 |
| Ca2 | Circular | 36.6 | 50 | Carbon steel | 114 × 2.19 × 342 | 335.7 | 671.5 | 2.25 | 1.22 | 9.38 |
| Cb0 | Circular | 42.7 | 0 | Carbon steel | 165 × 2.57 × 495 | 343.1 | 1436.0 | 1.97 | 1.07 | 0 |
| Cb1 | Circular | 41.8 | 25 | Carbon steel | 165 × 2.57 × 495 | 343.1 | 1422.0 | 1.99 | 1.10 | 0.97 |
| Cb2 | Circular | 36.6 | 50 | Carbon steel | 165 × 2.57 × 495 | 343.1 | 1401.5 | 2.24 | 1.13 | 2.40 |
| Cc0 | Circular | 42.7 | 0 | Carbon steel | 219 × 2.86 × 657 | 350.4 | 2158.0 | 1.68 | 1.08 | 0 |
| Cc1 | Circular | 41.8 | 25 | Carbon steel | 219 × 2.86 × 657 | 350.4 | 2101.0 | 1.67 | 1.09 | 2.64 |
| Cc2 | Circular | 36.6 | 50 | Carbon steel | 219 × 2.86 × 657 | 350.4 | 1982.0 | 1.80 | 1.09 | 8.16 |
| Sa0 | Square | 42.7 | 0 | Carbon steel | 100 × 1.94 × 300 | 388.1 | 666.0 | 2.48 | 1.43 | 0 |
| Sa1 | Square | 41.8 | 25 | Carbon steel | 100 × 1.94 × 300 | 388.1 | 652.5 | 2.48 | 1.09 | 2.03 |
| Sa2 | Square | 36.6 | 50 | Carbon steel | 100 × 1.94 × 300 | 388.1 | 619.0 | 2.69 | 1.52 | 7.06 |
| Sb0 | Square | 42.7 | 0 | Carbon steel | 150 × 2.94 × 450 | 344.4 | 1306.0 | 2.16 | 1.27 | 0.00 |
| Sb1 | Square | 41.8 | 25 | Carbon steel | 150 × 2.94 × 450 | 344.4 | 1283.0 | 2.17 | 1.30 | 1.76 |
| Sb2 | Square | 36.6 | 50 | Carbon steel | 150 × 2.94 × 450 | 344.4 | 1271.5 | 2.46 | 1.34 | 2.64 |
| Sc0 | Square | 42.7 | 0 | Carbon steel | 200 × 3.73 × 600 | 330.1 | 2295.0 | 2.14 | 1.01 | 0.00 |
| Sc1 | Square | 41.8 | 25 | Carbon steel | 200 × 3.73 × 600 | 330.1 | 2180.5 | 2.08 | 1.01 | 4.99 |
| Sc2 | Square | 36.6 | 50 | Carbon steel | 200 × 3.73 × 600 | 330.1 | 2119.0 | 2.30 | 1.03 | 7.67 |
| Yang and Ma [23] | | | | | | | | | | |
| C-S-N | Circular | 63.4 | 0 | Stainless steel | 120 × 1.77 × No data | 286.7 | 823.2 | 1.38 | 1.09 | 0 |
| C-S-C1 | Circular | 59.7 | 25 | Stainless steel | 120 × 1.77 × No data | 286.7 | 813.8 | 1.45 | 1.09 | 1.14 |
| C-S-C2 | Circular | 57.3 | 50 | Stainless steel | 120 × 1.77 × No data | 286.7 | 802.2 | 1.49 | 1.10 | 2.55 |
| C-S-C3 | Circular | 56.9 | 75 | Stainless steel | 120 × 1.77 × No data | 286.7 | 774.3 | 1.45 | 1.14 | 5.94 |
| C-S-F1 | Circular | 58.6 | 25 | Stainless steel | 120 × 1.77 × No data | 286.7 | 806.7 | 1.47 | 1.13 | 2.00 |
| C-S-F2 | Circular | 56.2 | 50 | Stainless steel | 120 × 1.77 × No data | 286.7 | 768.4 | 1.46 | 1.17 | 6.66 |
| C-S-F3 | Circular | 55.3 | 75 | Stainless steel | 120 × 1.77 × No data | 286.7 | 777.2 | 1.50 | 1.22 | 5.59 |
| S-S-N | Square | 63.4 | 0 | Stainless steel | 120 × 1.77 × No data | 286.7 | 923.4 | 1.55 | 0.92 | 0 |
| S-S-C1 | Square | 59.7 | 25 | Stainless steel | 120 × 1.77 × No data | 286.7 | 871.5 | 1.56 | 0.91 | 5.62 |
| S-S-C2 | Square | 57.3 | 50 | Stainless steel | 120 × 1.77 × No data | 286.7 | 848.5 | 1.58 | 0.90 | 8.11 |
| S-S-C3 | Square | 56.9 | 75 | Stainless steel | 120 × 1.77 × No data | 286.7 | 830.0 | 1.55 | 0.93 | 10.11 |
| S-S-F1 | Square | 58.6 | 25 | Stainless steel | 120 × 1.77 × No data | 286.7 | 857.1 | 1.56 | 0.96 | 7.18 |
| S-S-F2 | Square | 56.2 | 50 | Stainless steel | 120 × 1.77 × No data | 286.7 | 826.9 | 1.57 | 0.96 | 10.45 |
| S-S-F3 | Square | 55.3 | 75 | Stainless steel | 120 × 1.77 × No data | 286.7 | 831.1 | 1.60 | 0.95 | 10.00 |
| Shi et al. [24] | | | | | | | | | | |
| C0-1 | Circular | 42.6 | 0 | Carbon steel | 114 × 1.74 × 397 | 300.3 | 650.0 | 1.87 | – | 0 |
| C1-1 | Circular | 43.4 | 25 | Carbon steel | 114 × 1.80 × 395 | 300.3 | 655.0 | 1.85 | – | −0.77 |
| C1-2 | Circular | 43.4 | 25 | Carbon steel | 114 × 1.80 × 401 | 300.3 | 651.0 | 1.84 | – | −0.15 |
| C2-1 | Circular | 43.9 | 50 | Carbon steel | 114 × 1.84 × 396 | 300.3 | 636.0 | 1.77 | – | 2.15 |
| C2-2 | Circular | 43.9 | 50 | Carbon steel | 114 × 2.09 × 402 | 300.3 | 688.0 | 1.92 | – | −5.85 |
| C3-1 | Circular | 45.6 | 75 | Carbon steel | 114 × 2.05 × 394 | 300.3 | 635.0 | 1.71 | – | 2.31 |
| C3-2 | Circular | 45.6 | 75 | Carbon steel | 114 × 1.75 × 398 | 300.3 | 639.0 | 1.72 | – | 1.69 |
| C4-1 | Circular | 35.9 | 100 | Carbon steel | 114 × 1.71 × 400 | 300.3 | 557.0 | 1.90 | – | 14.31 |
| C4-2 | Circular | 35.9 | 100 | Carbon steel | 114 × 1.70 × 401 | 300.3 | 557.0 | 1.90 | – | 14.31 |
| S0-1 | Square | 42.6 | 0 | Carbon steel | 100 × 1.74 × 401 | 335.5 | 569.0 | 2.13 | – | 0 |
| S1-1 | Square | 43.4 | 25 | Carbon steel | 100 × 1.90 × 400 | 335.5 | 599.0 | 2.20 | – | −5.27 |
| S1-2 | Square | 43.4 | 25 | Carbon steel | 100 × 1.91 × 402 | 335.5 | 586.0 | 2.15 | – | −2.99 |
| S2-1 | Square | 43.9 | 50 | Carbon steel | 100 × 1.94 × 394 | 335.5 | 560.0 | 2.03 | – | 1.58 |
| S2-2 | Square | 43.9 | 50 | Carbon steel | 100 × 1.96 × 397 | 335.5 | 581.0 | 2.11 | – | −2.11 |
| S3-1 | Square | 45.6 | 75 | Carbon steel | 100 × 1.80 × 395 | 335.5 | 570.0 | 1.99 | – | −0.18 |
| S3-2 | Square | 45.6 | 75 | Carbon steel | 100 × 1.92 × 399 | 335.5 | 558.0 | 1.95 | – | 1.93 |
| S4-1 | Square | 35.9 | 100 | Carbon steel | 100 × 1.90 × 398 | 335.5 | 495.0 | 2.19 | – | 13.01 |
| S4-2 | Square | 35.9 | 100 | Carbon steel | 100 × 1.90 × 400 | 335.5 | 528.0 | 2.34 | – | 7.21 |
| Xiao et al. [25] | | | | | | | | | | |
| RCFS-0 | Circular | 47.2 | 0 | Carbon steel | 199.3 × 3.63 × 400 | 465.0 | 2513.0 | 2.13 | 1.57 | 0 |
| RCFS-30 | Circular | 42.4 | 30 | Carbon steel | 199.3 × 3.63 × 400 | 465.0 | 2332.0 | 2.20 | – | 7.20 |
| RCFS-50 | Circular | 45.7 | 50 | Carbon steel | 199.3 × 3.63 × 400 | 465.0 | 2299.0 | 2.02 | 1.50 | 8.52 |
| RCFS-70 | Circular | 36.7 | 70 | Carbon steel | 199.3 × 3.63 × 400 | 465.0 | 2182.0 | 2.38 | – | 13.17 |
| RCFS-100 | Circular | 38.9 | 100 | Carbon steel | 199.3 × 3.63 × 400 | 465.0 | 2210.0 | 2.28 | 1.67 | 12.06 |
| Wang et al. [26] | | | | | | | | | | |
| cfst8-L35-0 | Circular | 50.6 | 0 | Carbon steel | 140 × 2.71 × 420 | 309.0 | 1115.0 | 1.79 | 2.12 | 0 |
| cfst8-L35-0.5 | Circular | 46.9 | 50 | Carbon steel | 140 × 2.78 × 420 | 309.0 | 1113.0 | 1.93 | 2.25 | 0.18 |
| cfst8-L35-1 | Circular | 45.3 | 100 | Carbon steel | 140 × 2.72 × 420 | 309.0 | 1106.0 | 1.98 | 2.53 | 0.81 |
| cfst12-L35-0 | Circular | 50.6 | 0 | Carbon steel | 140 × 3.87 × 420 | 335.3 | 1520.0 | 2.44 | 2.69 | 0 |
| cfst12-L35-0.5 | Circular | 46.9 | 50 | Carbon steel | 140 × 3.84 × 420 | 335.3 | 1390.0 | 2.41 | 2.76 | 8.55 |
| cfst12-L35-1 | Circular | 45.3 | 100 | Carbon steel | 140 × 3.88 × 420 | 335.3 | 1428.0 | 2.56 | 3.27 | 6.05 |
| cfst15-L35-0 | Circular | 50.6 | 0 | Carbon steel | 133 × 4.57 × 400 | 302.0 | 1336.0 | 2.38 | 2.53 | 0 |
| cfst15-L35-0.5 | Circular | 46.9 | 50 | Carbon steel | 133 × 4.61 × 400 | 302.0 | 1383.0 | 2.65 | 3.00 | −3.52 |
| cfst15-L35-1 | Circular | 45.3 | 100 | Carbon steel | 133 × 4.60 × 400 | 302.0 | 1377.0 | 2.73 | 3.18 | −3.07 |
| Tam et al. [27] | | | | | | | | | | |
| CC-0 | Circular | 41.2 | 0 | Carbon steel | 139.1 × 2.79 × 420 | 388.5 | 1211.6 | 2.42 | 1.75 | 0 |
| CC-25 | Circular | 41.7 | 25 | Carbon steel | 138.6 × 2.79 × 420 | 388.5 | 1175.1 | 2.33 | 1.70 | 3.01 |

(*continued on next page*)

**Table 3** (*continued*)

| Specimen | Section | $f_{cu}$ (MPa) | $r$ (%) | Tube type | $D$ (or $B$) × $t$ × $L$ (mm) [a] | $f_y$ (MPa) | $N_{ue}$ (kN) [a] | fcc/fc | Ess/Ec | SI [a] |
|---|---|---|---|---|---|---|---|---|---|---|
| CC-50 | Circular | 41.0 | 50 | Carbon steel | 138.7 × 2.79 × 420 | 388.5 | 1212.5 | 2.45 | 1.66 | −0.07 |
| CC-100 | Circular | 37.8 | 100 | Carbon steel | 138.0 × 2.79 × 420 | 388.5 | 1147.5 | 2.54 | 1.63 | 5.29 |
| CS-0 | Circular | 41.2 | 0 | Stainless steel | 168.9 × 2.86 × 510 | 339.6 | 1707.5 | 2.31 | 1.52 | 0 |
| CS-25 | Circular | 41.7 | 25 | Stainless steel | 168.4 × 2.86 × 510 | 339.6 | 1595.1 | 2.15 | 1.53 | 6.58 |
| CS-50 | Circular | 41.0 | 50 | Stainless steel | 169.7 × 2.86 × 510 | 339.6 | 1607.4 | 2.17 | 1.46 | 5.86 |
| CS-100 | Circular | 37.8 | 100 | Stainless steel | 170.6 × 2.86 × 510 | 339.6 | 1573.1 | 2.28 | 1.31 | 7.87 |
| RC-0 | Square | 41.2 | 0 | Carbon steel | (197.8,98.5)×3.83 × 600 | 480.2 | 1612.8 | 2.51 | 2.07 | 0 |
| RC-25 | Square | 41.7 | 25 | Carbon steel | (199.8,99.9)×3.83 × 600 | 480.2 | 1609.5 | 2.42 | 1.89 | 0.20 |
| RC-50 | Square | 41.0 | 50 | Carbon steel | (199.4,99.2)×3.83 × 600 | 480.2 | 1608.2 | 2.48 | 1.87 | 0.29 |
| RC-100 | Square | 37.8 | 100 | Carbon steel | (200.0,98.7)×3.83 × 600 | 480.2 | 1567.0 | 2.63 | 1.77 | 2.84 |
| RS-0 | Square | 41.2 | 0 | Stainless steel | (200.7,97.1)×3.96 × 600 | 301.5 | 1422.9 | 2.22 | 1.86 | 0 |
| RS-25 | Square | 41.7 | 25 | Stainless steel | (200.2,98.5)×3.96 × 600 | 301.5 | 1350.2 | 2.05 | 1.76 | 5.11 |
| RS-50 | Square | 41.0 | 50 | Stainless steel | (200.7,97.9)×3.96 × 600 | 301.5 | 1388.7 | 2.15 | 1.74 | 2.40 |
| RS-100 | Square | 37.8 | 100 | Stainless steel | (200.2,98.9)×3.96 × 600 | 301.5 | 1291.8 | 2.16 | 1.57 | 9.21 |

[a] $N_{ue}$ is the experimentally obtained ultimate axial load.

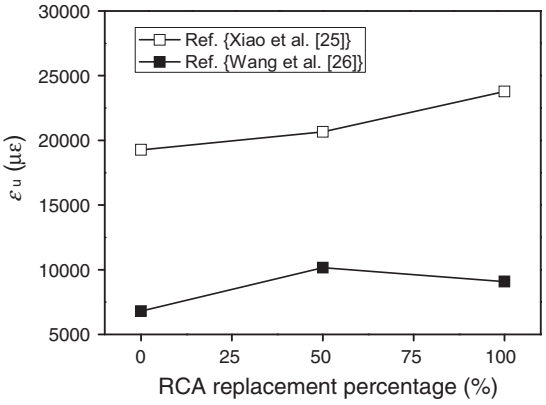


**Fig. 6.** Effect of RCA content on peak strain of RACFST.

a jacketed material. The use of stainless steel tubes and/or epibolic stainless steel plates also offers the advantages of aesthetics and durability. Yang and Ma [23] carried out an experimental investigation on the behavior of recycled aggregate concrete-filled stainless steel tube beams subjected to four-point bending. Table 2 lists the details of beam test specimens and the corresponding test results. The experimental results showed that recycled aggregate concrete-filled stainless steel tube beams exhibited similar failure pattern as the corresponding natural aggregate concrete-filled stainless steel tube beams, and the RCA replacement percentage has little effect on the failure pattern as shown in Fig. 5.

It can be observed from Fig. 5 that the failure pattern of the stainless steel tubes that involves multiple local buckling locations in the compression area is similar to that of the aforementioned carbon steel tubes. Based on the average strain measured in the cross-section, Yang and Ma reported that the reduction in initial section flexural stiffness, serviceability-level section flexural stiffness and bending moment capacity for the recycled aggregate concrete-filled stainless steel tube beams were 2.7–19.7%, 3.5–15.6% and 1.3–10.5%, respectively.

### 3.2. RACFST stub columns under axial compression

Many researchers such as Konno et al. [12], Yang and Han [22], Yang and Ma [23], Shi et al. [24], Xiao et al. [25] and Wang et al. [26] performed experimental studies on the behavior of RACFST stub columns under axial compression. Their test results listed in Table 3 have collectively shown that, on the material level, both strength (axial compressive strength enhancement $f_{cc}/f_c$) and stiffness (elasticity modulus enhancement $E_{sc}/E_c$) of RAC improve due to the confinement of concrete and the strength contribution by steel tubes; and on the structural level, the ultimate strength (strength index SI shown in Table 3) of RAC decreases while the corresponding strain (see Fig. 6) increases when the replacement content of RCA is increased. As for the failure mode of RACFST, it is observed that replacing natural coarse aggregates with recycled ones does not affect the failure mode for CFST stub columns. In Ref. [25], Xiao et al. conducted a series of tests to study the axial compressive performance of recycled aggregate concrete-filled glass fiber reinforced polymer (GFRP) tubes, and it can be found from Fig. 7 that the mechanical properties (peak load, ultimate strain and stiffness) of RAC confined by steel tubes are better than those of RAC confined by GFRP tubes when all parameters are kept the same.

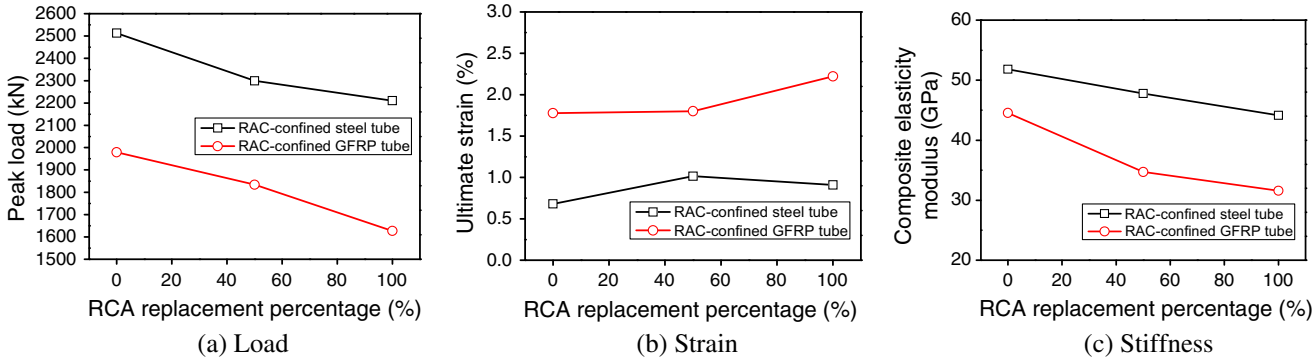


**Fig. 7.** Comparison of mechanical indices between RACFST and RACFST strengthened by CFRP (Xiao et al. [25]).

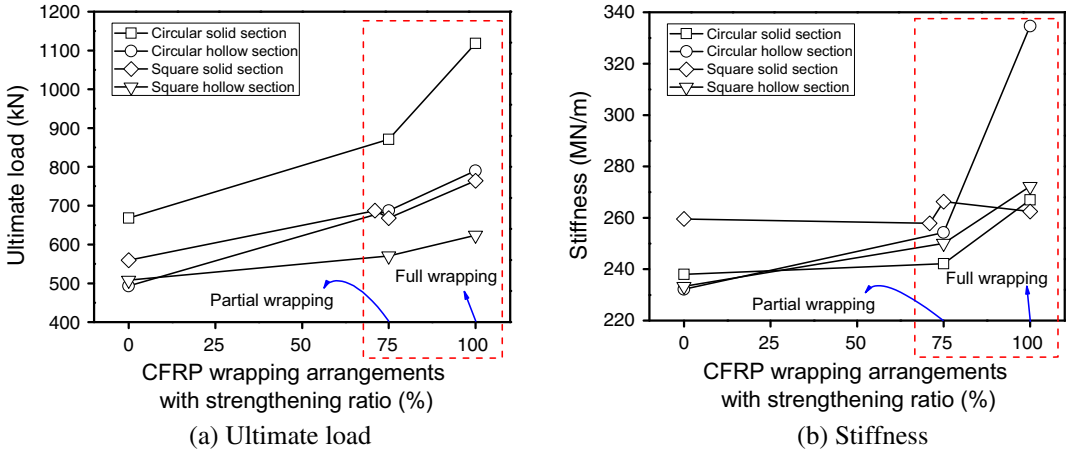


**Fig. 8.** Effect of CFRP wrapping arrangements on mechanical indices of CFRP strengthening RACFST (Dong et al. [30]).

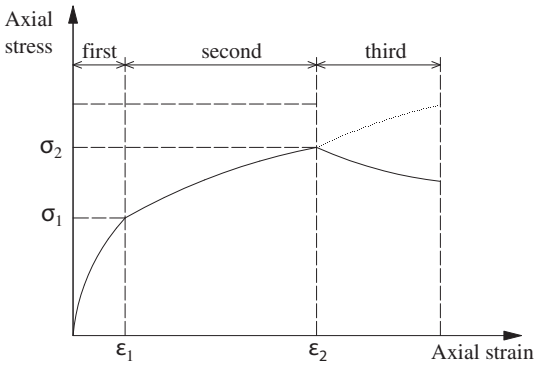


**Fig. 9.** The stress-strain relationship of confining RAC (Huang et al. [31]).

With an aim toward combining the advantages of RAC and stainless steel, Tam et al. [27] reported that the failure mode of recycled coarse aggregate-filled stainless steel tube stub columns was similar to that of conventional concrete-filled stainless steel tube stub columns. Both the RAC and conventional concrete-filled stainless steel tube stub columns failed by local buckling, which resembles the failure pattern observed in previous studies [28,29].

Details of the stub column specimens and the test loads reported by Yang and Han [22], Yang and Ma [23], Shi et al. [24], Xiao et al. [25], Wang et al. [26] and Tam et al. [27] are summarized in Table 3.

In addition, RACFST columns can be strengthened by fiber reinforced polymer (FRP) jackets. Dong et al. [30] adopted this idea and evaluated the axial compressive behavior of recycled aggregate concrete-filled steel tube stub columns strengthened by carbon fiber reinforced polymer (CFRP). The relationship between mechanical indices (strength and stiffness) and CFRP wrapping arrangements with strengthening ratio are shown in Fig. 8. Hence, the results indicate that the use of CFRP wrapping for strengthening RACFST gives significant enhancement to the load carrying capacity and stiffness. Furthermore, it was found that the use of full wrapping arrangement of CFRP was more effective than the partial wrapping arrangement in terms of enhancing the load carrying capacity and stiffness of the steel tube columns.

### 3.2.1. Theoretical studies of RACFST columns

In addition to experimental studies, theoretical investigations on the behavior of RACFST have been carried out by a number of researchers. Huang et al. [31] performed theoretical study on the mechanical response of recycled aggregate concrete confined by steel tubes under axial compression to examine the sensitivity of confining pressure on the strength and the deformation of RAC. The assumption of constant confinement or elastic–plastic confinement is not appropriate for concrete confined by steel tubes, and the RCA replacement percentage has a moderate effect on the mechanical response of the confined concrete. Hence, the axial stress-strain relationship of the confined RAC in RACFST can be characterized by three stages with respect to the variations of the confining pressure. These stages are shown in Fig. 9 with respect to the axial stress-axial strain and confining pressure-axial strain of the confining concrete. The analytical model for the confining RAC in RACFST can be obtained when the key points and the constitutive relationship are determined. The model can be expressed as following:

(1) The first stage:

$$\begin{aligned}
\sigma(\varepsilon) &= \frac{\varepsilon}{\varepsilon_1}\cdot\frac{a\cdot\sigma_1}{a-1+(\varepsilon/\varepsilon_1)^a} \quad \varepsilon \leqslant \varepsilon_1 \\
a &= \frac{E_c}{E_c-\sigma_1/\varepsilon_1} \\
\sigma_1 &= f_c[1+2.7\cdot(p_1/f_c)], \\
\varepsilon_1 &= (-0.0475r+1.0624)\cdot(0.833+0.121\sqrt{f_{cu}}) \\
&\quad \cdot 10^{-3}(0.7\leqslant r\leqslant 1.0), \\
\varepsilon_1 &= \varepsilon_c' \quad (0.7\leqslant r\leqslant 1.0).
\end{aligned} \tag{1}$$

(2) The second stage:

$$\begin{aligned}
\sigma(\varepsilon) &= (\sigma_2-\sigma_1)\cdot\frac{\ln(\varepsilon/\varepsilon_1)}{\ln(\varepsilon_2/\varepsilon_1)}+\sigma_1 \quad \varepsilon_1<\varepsilon\leqslant\varepsilon_2, \\
\sigma_2 &= f_c\{1+2.7\cdot[1.6tf_y/(Df_c)]\cdot(28/f_{cu})^{0.15}\}, \\
\varepsilon_2 &= \varepsilon_1\cdot 5\left[\left(\frac{\sigma_2}{f_c}\right)^{0.8}-0.8\right].
\end{aligned} \tag{2}$$

(3) The third stage:

$$\begin{aligned}
\sigma(\varepsilon) &= \sigma_2\cdot\frac{\xi_r^{0.75}}{2+\xi_r}\cdot\left[\left(\frac{\varepsilon}{\varepsilon_2}\right)^{0.1\xi_r}-1\right]+\sigma_1, \quad (\xi_r>1.12)\varepsilon_2<\varepsilon, \\
\sigma(\varepsilon) &= \frac{\sigma_2\cdot(\varepsilon/\varepsilon_2)}{\{\beta\cdot[(\varepsilon/\varepsilon_2)-1]^2+(\varepsilon/\varepsilon_2)\}}, \quad (\xi_r\leqslant 1.12)\varepsilon_2<\varepsilon, \\
\beta &= (2.36.10^{-3})^{0.25+(\varepsilon_r-0.5)^7}\cdot(f_c)^2\cdot 3.5\cdot 10^{-4}
\end{aligned} \tag{3}$$

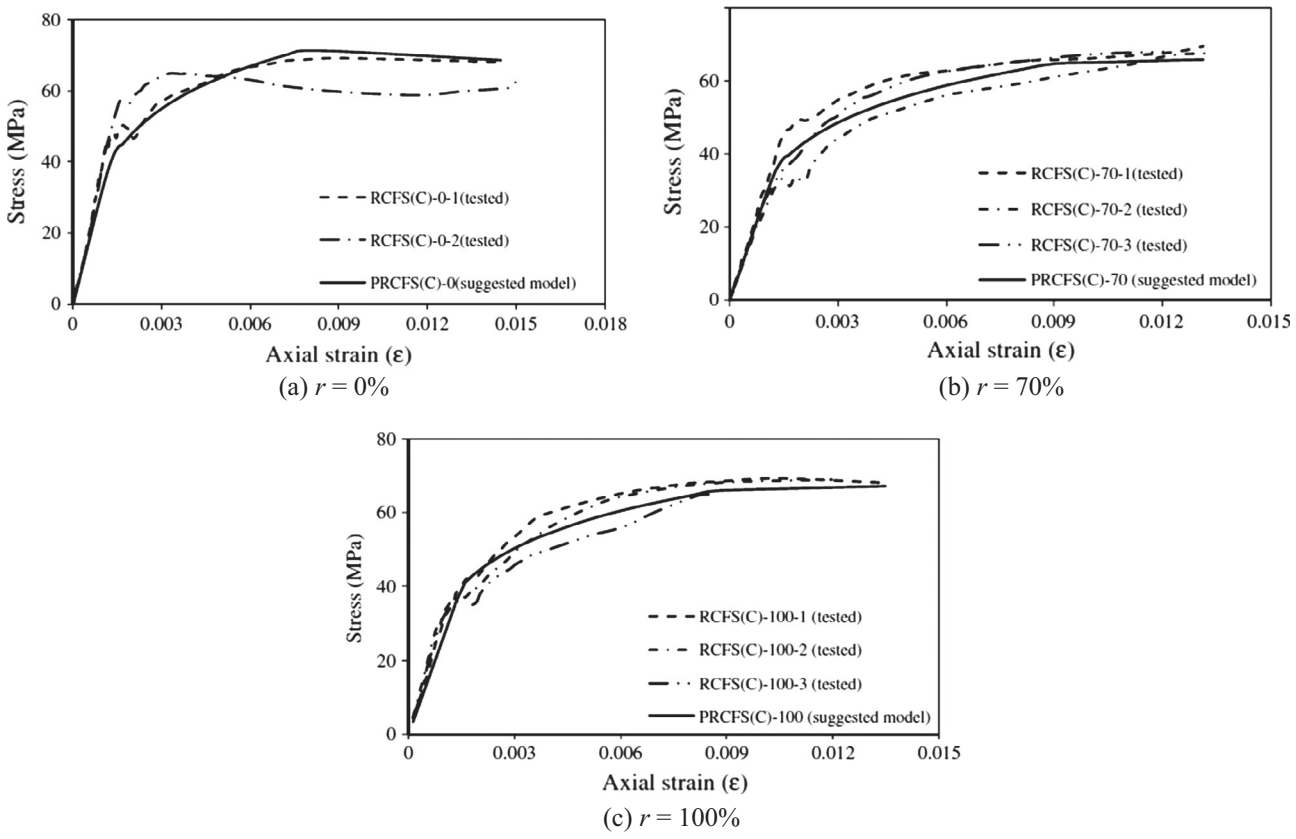


**Fig. 10.** Comparison of test results and the calculated results (Huang et al. [31]).

where $p_1$ is the confining pressure, and $p_1$ can be expressed as $p_1 = 2t\sigma_{1h}/D$; $\sigma_{1h}$ is the hoop stress of steel at the first keypoint; $D$ is the diameter of outer tube, $t$ is the thickness of outer tube; $E_c$ is the elastic modules of RAC, $f_c$ is the axial compressive strength of RAC prism, $f_{cu}$ is the axial compressive strength of RAC cube; $f_y$ is the tensile strength of outer tube; $\xi_r = f_y A_s/(f_c A_c)$.

Based on the above-listed theoretical expressions of axial loaded RACFST, the comparison of test results and calculated results is shown in Fig. 10.

Liu et al. [32] proposed a damage model based on damage mechanics to evaluate the damage progression of RACFST subjected to axial loads. In this study, the recycled aggregate concrete and the conventional concrete were idealized to be shunt-wound and series-wound springs in the vertical and transverse directions as shown in Fig. 11.

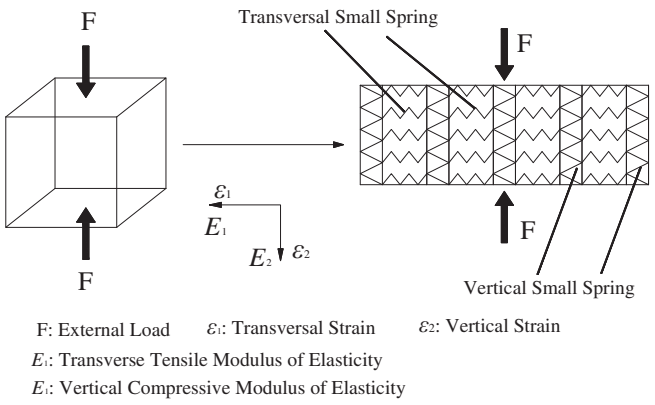


**Fig. 11.** Simplified model of RAC and ordinary concrete under axial compression (Liu et al. [32]).

If the section height of concrete is denoted as $H_1$ and the number of coarse aggregates in that section of concrete is denoted as $N_1$, the initial concrete damage $D_{0o}$ and the initial RAC damage $D_{0r}$ can be expressed as

$$D_{0o} = 0.5 \times 2 \times \delta \times N_1/H_1 \tag{4}$$

$$D_{0r} = 4 \times 0.5 \times 2 \times \delta \times N_1/H_1 \tag{5}$$

The load-displacement curves and stress-strain curves of the samples of CFST and RCFST are displayed in Fig. 12. Based on the theoretical and experimental studies, Liu et al. [32] found that the energy absorbing capacity of recycled concrete is worse than that of ordinary concrete, because the initial damage of recycled concrete is more than that of the latter, which is verified by experiments. For RACFST and CFST, the initial damage of recycled concrete and ordinary concrete does not continue to grow, attributing to the tightening-ring force of steel tube. The energy-absorbing capacity of RACFST in the elastic range is much more than that of recycled concrete in the elastic range, and their ratio calculated based on the damage mechanics model in this paper is in agreement with the experimental results.

### 3.2.2. Geopolymeric recycled concrete

Geopolymeric recycled concrete (GRC) is a new construction material which takes environmental sustainability into account. In GRC, cement is completely substituted by alkali solution and fly ash, and the natural coarse aggregates are replaced by recycled coarse aggregates either partially or totally. Shi et al. [33] investigated the structural behavior of geopolymeric recycled concrete-filled steel tube (GRCFST) stub columns under axial compression. Two different square hollow sections of carbon steel tubes (type I: 150 mm × 150 mm × 5 mm, and type II: 200 mm × 200 mm

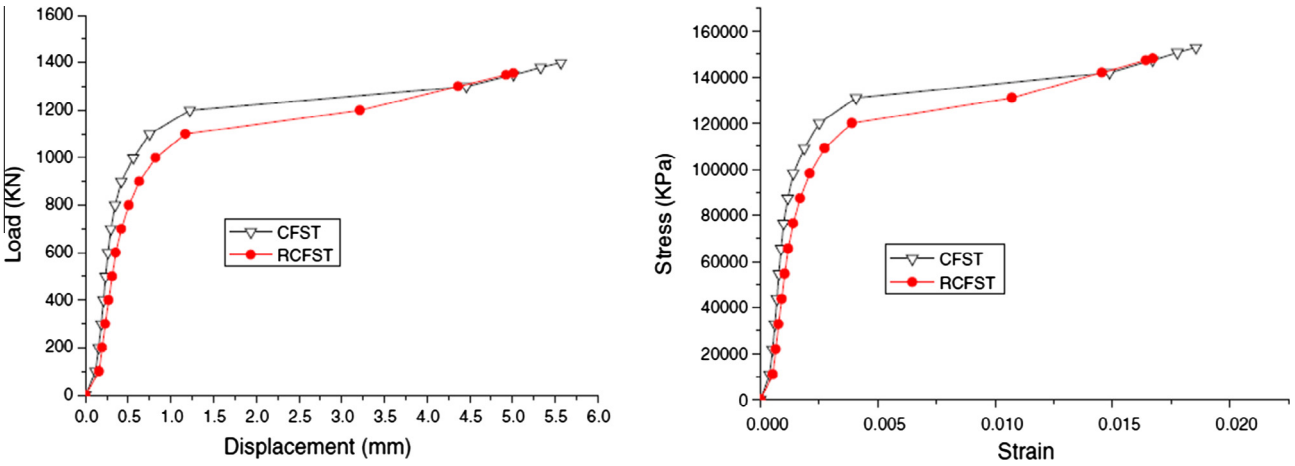


**Fig. 12.** Load-displacement curves and stress–strain curves of tested RCFST and CFST (Liu et al. [32]).

**Table 4**
Concentrically loaded GRC specimens.

| Specimen | Section | $f_{cu}$ (MPa) | RCA source | $r$ (%) | Tube type | $D$ (or $B$) × $t$ × $L$ (mm) | $f_y$ (MPa) | $N_{ue}$ (kN) [a] | SI (%) |
|---|---|---|---|---|---|---|---|---|---|
| S1RAC0 | Square | 79.0 | – | 0 | Carbon steel | 200 × 6 × 750 | 467.0 | 3561 | 0 |
| S1RAC50 | Square | 66.3 | Waste concrete | 50 | Carbon steel | 200 × 6 × 751 | 467.0 | 3466 | 2.67 |
| S1RAC100 | Square | 58.1 | Waste concrete | 100 | Carbon steel | 200 × 6 × 752 | 467.0 | 3297 | 7.41 |
| S1GRC0 | Square | 80.2 | Geopolymer | 0 | Carbon steel | 200 × 6 × 753 | 467.0 | 4497 | 0 |
| S1GRC50 | Square | 65.1 | Geopolymer | 50 | Carbon steel | 200 × 6 × 754 | 467.0 | 3380 | 24.84 |
| S1GRC100 | Square | 51.2 | Geopolymer | 100 | Carbon steel | 200 × 6 × 755 | 467.0 | 3376 | 24.93 |
| S2RAC0 | Square | 79.0 | – | 0 | Carbon steel | 150 × 5 × 755 | 486.0 | 2184 | 0 |
| S2RAC50 | Square | 66.3 | Waste concrete | 50 | Carbon steel | 150 × 5 × 755 | 486.0 | 2100 | 3.85 |
| S2RAC100 | Square | 58.1 | Waste concrete | 100 | Carbon steel | 150 × 5 × 755 | 486.0 | 1947 | 10.85 |
| S2GRC0 | Square | 80.2 | Geopolymer | 0 | Carbon steel | 150 × 5 × 755 | 486.0 | 2676 | 0 |
| S2GRC50 | Square | 65.1 | Geopolymer | 50 | Carbon steel | 150 × 5 × 755 | 486.0 | 2100 | 21.52 |
| S2GRC100 | Square | 51.2 | Geopolymer | 100 | Carbon steel | 150 × 5 × 755 | 486.0 | 2057 | 23.13 |

[a] $N_{ue}$ is the experimentally obtained ultimate axial load.

× 6 mm) filled with GRC and recycled aggregate concrete (RAC) and with recycled aggregate replacement percentages of 0%, 50% and 100%, were used in the tests. Detailed information about the specimens and the test loads are given in Table 4. The test results show that the load capacities of GRCFST columns decrease with increasing recycled aggregate replacement percentages, so do RACFST columns; and the ductility of the columns under axial loading is improved by the presence of recycled aggregates. However, the most important finding is that the influence of recycled aggregates on the strength and ductility of GRCFST columns is generally greater than those of RACFST columns.

*3.2.3. Effect of pre-wetting*

It should be noted that in the aforementioned experimental and theoretical research, the recycled coarse aggregates used in manufacturing RACFST were all pre-soaked due to the strong water-absorbing capacity of recycled coarse aggregates. This means that the actual $w/c$ in RAC is higher than the design $w/c$. With an increase in RCA content and hence a higher $w/c$, it was postulated that the strength decreasing aspect of RAC at the material level can lead to a lower load carrying capacity for RACFST at the structural level. To test this hypothesis, Chen et al. [34] conducted tests on the effect of RCA replacement percentages on the behavior of RACFST stub columns under axial compression in which the recycled coarse aggregates used were not pre-wetted. Table 5 presents the details of the specimens. Fig. 13 shows the typical failure modes of RACFST stub columns after axial compression. It was concluded that while the failure mode of RACFST columns was still similar to that of conventional CFST columns, the peak stress of RACFST stub columns was higher and the corresponding strain of these stub columns was lower with an increasing RCA replacement percentage (see Fig. 14). The main reason that a higher peak stress and a lower corresponding strain are obtained can be attributed to a reduction of the actual $w/c$ in RAC, which leads to lower water content and denser the cementitious matrix in concrete.

All these research have shown that RAC is a viable alternative to NAC for use in composite structural members.

*3.3. RACFST columns under eccentric load*

Yang and Han [35] tested and evaluated the behavior of RACFST columns under eccentric load by considering the variation of tube shapes (circular and square), RCA replacement percentages (0%, 25% and 50%) and load eccentricity ratios (from 0 to 0.53). Table 6 gives the details of the specimens and the corresponding test loads. Within the scope of their study, the following conclusions can be drawn:

- The typical failure modes of RACFST columns are similar to those of the conventional CFST columns. They are all related to buckling.
- The ultimate load carrying capacities of composite columns decrease with an increase in the load eccentricity ratios. This has also been confirmed in previous studies of CFST.
- The ultimate load carrying capacities of conventional concrete-filled circular steel tube columns are 1.7–9.1% higher than those of circular columns with recycled aggregate concrete containing 25% RCA and 50% RCA; and for square columns, the ranges are

**Table 5**
Chen et al.'s test specimens.

| Specimen | Section | $f_{cu}$ (MPa) | RCA source | $r$ (%) | Tube type | $D$ (or $B$) × $t$ × $L$ (mm) | $f_y$ (MPa) | $N_{ue}$ (kN) [a] | SI (%) |
|---|---|---|---|---|---|---|---|---|---|
| CA-0 | Circular | 31.1 | – | 0 | Carbon steel | 88.34 × 2.59 × 285 | 342.7 | 504.4 | 0 |
| CA-1 | Circular | 29.1 | Waste concrete | 10 | Carbon steel | 88.20 × 2.60 × 286 | 342.7 | 517.5 | −2.61 |
| CA-2 | Circular | 28.2 | Waste concrete | 20 | Carbon steel | 88.20 × 2.67 × 286 | 342.7 | 509.7 | −1.05 |
| CA-3 | Circular | 32.4 | Waste concrete | 30 | Carbon steel | 88.24 × 2.55 × 286 | 342.7 | 522.2 | −3.54 |
| CA-4 | Circular | 33.8 | Waste concrete | 40 | Carbon steel | 88.02 × 2.44 × 284 | 342.7 | 521.7 | −3.44 |
| CA-5 | Circular | 31.5 | Waste concrete | 50 | Carbon steel | 88.20 × 2.54 × 286 | 342.7 | 519.9 | −3.08 |
| CA-6 | Circular | 30.3 | Waste concrete | 60 | Carbon steel | 88.20 × 2.43 × 287 | 342.7 | 517.2 | −2.55 |
| CA-7 | Circular | 35.9 | Waste concrete | 70 | Carbon steel | 88.30 × 2.54 × 285 | 342.7 | 530.9 | −5.25 |
| CA-8 | Circular | 37.0 | Waste concrete | 80 | Carbon steel | 88.10 × 2.51 × 286 | 342.7 | 533.1 | −5.70 |
| CA-9 | Circular | 34.3 | Waste concrete | 90 | Carbon steel | 88.14 × 2.40 × 283 | 342.7 | 538.1 | −6.68 |
| CA-10 | Circular | 38.4 | Waste concrete | 100 | Carbon steel | 88.32 × 2.51 × 284 | 342.7 | 541.0 | −7.25 |
| CB-0 | Circular | 31.1 | – | 0 | Carbon steel | 112.00 × 1.78 × 363 | 357.2 | 636.8 | 0 |
| CB-1 | Circular | 29.1 | Waste concrete | 10 | Carbon steel | 112.38 × 2.07 × 363 | 357.2 | 639.6 | −0.44 |
| CB-2 | Circular | 28.2 | Waste concrete | 20 | Carbon steel | 111.88 × 1.88 × 360 | 357.2 | 670.4 | −5.28 |
| CB-3 | Circular | 32.4 | Waste concrete | 30 | Carbon steel | 111.70 × 1.66 × 361 | 357.2 | 677.6 | −6.41 |
| CB-4 | Circular | 33.8 | Waste concrete | 40 | Carbon steel | 112.10 × 2.05 × 357 | 357.2 | 676.6 | −6.25 |
| CB-5 | Circular | 31.5 | Waste concrete | 50 | Carbon steel | 112.00 × 1.90 × 360 | 357.2 | 673.7 | −5.79 |
| CB-6 | Circular | 30.3 | Waste concrete | 60 | Carbon steel | 112.70 × 2.00 × 360 | 357.2 | 629.2 | 1.20 |
| CB-7 | Circular | 35.9 | Waste concrete | 70 | Carbon steel | 112.18 × 2.01 × 360 | 357.2 | 660.0 | −3.64 |
| CB-8 | Circular | 37.0 | Waste concrete | 80 | Carbon steel | 112.16 × 1.98 × 363 | 357.2 | 662.7 | −4.07 |
| CB-9 | Circular | 34.3 | Waste concrete | 90 | Carbon steel | 112.08 × 1.92 × 364 | 357.2 | 660.1 | −3.66 |
| CB-10 | Circular | 38.4 | Waste concrete | 100 | Carbon steel | 113.14 × 2.27 × 359 | 357.2 | 679.7 | −6.73 |
| SA-0 | Square | 35.2 | – | 0 | Carbon steel | 121 × 3.08 × 359 | 340.7 | 892.7 | 0 |
| SA-1 | Square | 33.0 | Waste concrete | 10 | Carbon steel | 121 × 3.25 × 359 | 340.7 | 915.9 | −2.60 |
| SA-2 | Square | 31.9 | Waste concrete | 20 | Carbon steel | 121 × 3.13 × 359 | 340.7 | 938.5 | −5.13 |
| SA-3 | Square | 36.7 | Waste concrete | 30 | Carbon steel | 121 × 3.06 × 359 | 340.7 | 960.0 | −7.54 |
| SA-4 | Square | 38.4 | Waste concrete | 40 | Carbon steel | 121 × 3.16 × 359 | 340.7 | 980.9 | −9.88 |
| SA-5 | Square | 35.7 | Waste concrete | 50 | Carbon steel | 121 × 3.20 × 359 | 340.7 | 945.5 | −5.91 |
| SA-6 | Square | 34.5 | Waste concrete | 60 | Carbon steel | 121 × 3.12 × 359 | 340.7 | 940.0 | −5.30 |
| SA-7 | Square | 40.7 | Waste concrete | 70 | Carbon steel | 121 × 3.07 × 359 | 340.7 | 943.6 | −5.70 |
| SA-8 | Square | 41.9 | Waste concrete | 80 | Carbon steel | 121 × 3.15 × 359 | 340.7 | 956.1 | −7.10 |
| SA-9 | Square | 39.0 | Waste concrete | 90 | Carbon steel | 121 × 3.13 × 359 | 340.7 | 972.5 | −8.94 |
| SA-10 | Square | 43.6 | Waste concrete | 100 | Carbon steel | 121 × 3.08 × 359 | 340.7 | 971.3 | −8.80 |

[a] $N_{ue}$ is the experimentally obtained ultimate axial load.


**Fig. 13.** Failure patterns of specimens (Chen et al. [34]).

1.4–13.5%. This is because the strength of the recycled aggregate concrete is lower than that of natural aggregate or conventional concrete.

In addition, Yang and Han [35] compared design formulas from six codes related to CFST to predict the load carrying capacity of RACFST. Their calculations showed that except for EC4 [36], which over-estimated the strength, ACI 318-99 [37], AIJ [38], AISC-LRFD [39], BS5400 [40] and DBJ13-51-2003 [41] all gave conservative results for predicting the strengths of recycled aggregate concrete-filled steel tube columns.

### 3.4. Long-term properties of RACFST columns

Long-term properties of recycled coarse aggregate have been investigated by various researchers [42–44]. One conclusion that can be made from these studies is that drying shrinkage and creep of RAC are significantly higher than those of natural aggregate

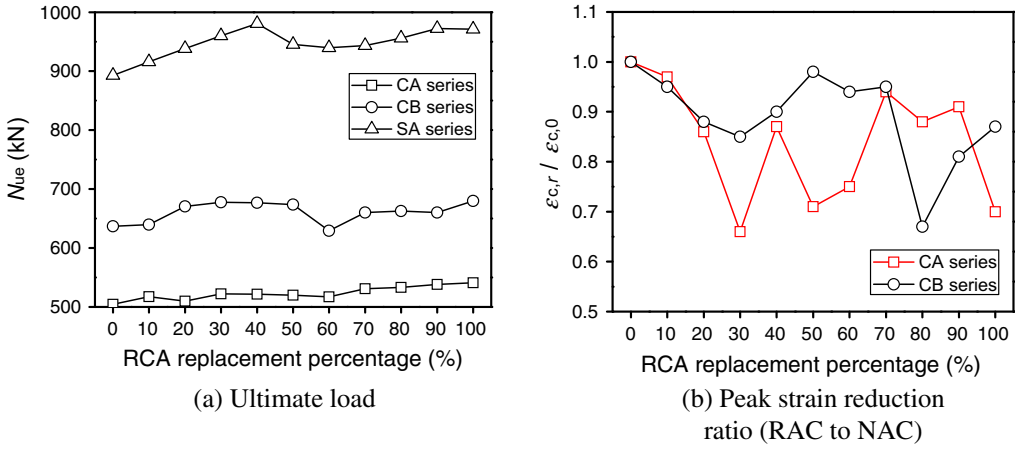


**Fig. 14.** Effect of RCA content on strength and deformation of RACFST without pre-wetting (Chen et al. [34]).

**Table 6**
Yang and Han's test specimens.

| Specimen | Section | $f_{cu}$ (MPa) | RCA source | $r$ (%) | Tube type | $D$ (or $B$) × $t$ × $L$ (mm) | $f_y$ (MPa) | $N_{ue}$ (kN) [a] | SI (%) |
|---|---|---|---|---|---|---|---|---|---|
| CA0 | Circular | 50.8 | – | 0 | Carbon steel | 165 × 2.57 × 1650 | 343.1 | 1217.0 | 0 |
| CA1 | Circular | 46.7 | Waste concrete | 25 | Carbon steel | 165 × 2.57 × 1650 | 343.1 | 1158.0 | 4.85 |
| CA2 | Circular | 44.1 | Waste concrete | 50 | Carbon steel | 165 × 2.57 × 1650 | 343.1 | 1106.5 | 9.08 |
| CB0 | Circular | 50.8 | – | 0 | Carbon steel | 165 × 2.57 × 1650 | 343.1 | 877.0 | 0 |
| CB1 | Circular | 46.7 | Waste concrete | 25 | Carbon steel | 165 × 2.57 × 1650 | 343.1 | 836.0 | 4.68 |
| CB2 | Circular | 44.1 | Waste concrete | 50 | Carbon steel | 165 × 2.57 × 1650 | 343.1 | 800.0 | 8.78 |
| CC0 | Circular | 50.8 | – | 0 | Carbon steel | 165 × 2.57 × 1650 | 343.1 | 615.0 | 0 |
| CC1 | Circular | 46.7 | Waste concrete | 25 | Carbon steel | 165 × 2.57 × 1650 | 343.1 | 604.5 | 1.71 |
| CC2 | Circular | 44.1 | Waste concrete | 50 | Carbon steel | 165 × 2.57 × 1650 | 343.1 | 601.0 | 2.28 |
| SA0 | Square | 50.8 | – | 0 | Carbon steel | 150 × 2.94 × 1732 | 344.4 | 1285.0 | 0 |
| SA1 | Square | 46.7 | Waste concrete | 25 | Carbon steel | 150 × 2.94 × 1732 | 344.4 | 1266.5 | 1.44 |
| SA2 | Square | 44.1 | Waste concrete | 50 | Carbon steel | 150 × 2.94 × 1732 | 344.4 | 1248.5 | 2.84 |
| SB0 | Square | 50.8 | – | 0 | Carbon steel | 150 × 2.94 × 1732 | 344.4 | 910.0 | 0 |
| SB1 | Square | 46.7 | Waste concrete | 25 | Carbon steel | 150 × 2.94 × 1732 | 344.4 | 858.5 | 5.66 |
| SB2 | Square | 44.1 | Waste concrete | 50 | Carbon steel | 150 × 2.94 × 1732 | 344.4 | 830.0 | 8.79 |
| SC0 | Square | 50.8 | – | 0 | Carbon steel | 150 × 2.94 × 1732 | 344.4 | 740.0 | 0 |
| SC1 | Square | 46.7 | Waste concrete | 25 | Carbon steel | 150 × 2.94 × 1732 | 344.4 | 659.0 | 10.95 |
| SC2 | Square | 44.1 | Waste concrete | 50 | Carbon steel | 150 × 2.94 × 1732 | 344.4 | 640.0 | 13.51 |

[a] $N_{ue}$ is the experimentally obtained ultimate axial load.

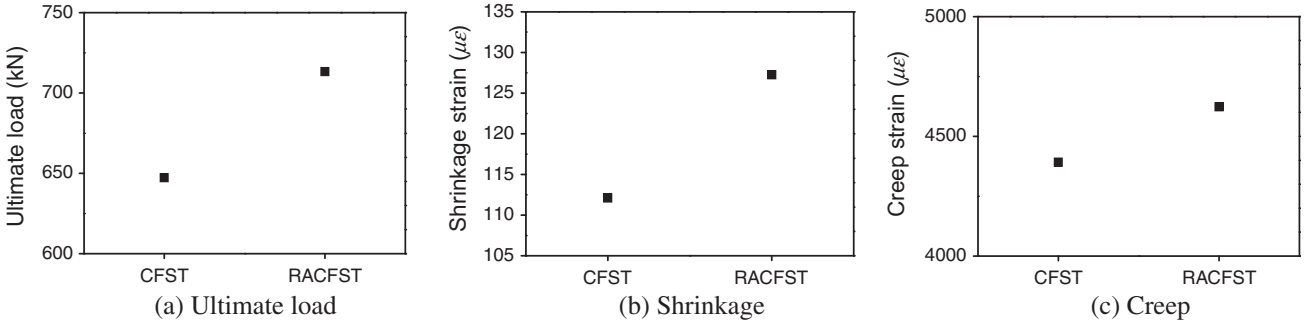


**Fig. 15.** Comparison of test results and the calculated results (Huang et al. [31]).

concrete (NAC). Yang et al. [45] reported that while the time history of concrete shrinkage and creep in RACFST columns was similar to those of the corresponding conventional CFST columns, the shrinkage and creep strains of RACFST columns were higher when compared with conventional CFST columns. In addition, Yang et al. [45] found that the ACI committee 209 [46] calibrated model could be used to predict the total final shrinkage and final creep coefficient for RAC.

In a study by Yang [47], the effect of RCA replacement percentages on the long-term load carrying capacities and long-term deformations (shrinkage and creep) of RACFST columns was presented. It was found from Fig. 15 that the long-term load carrying capacity and deformations of RACFST columns are larger than those of conventional CFST columns. Also, it can be observed Fig. 16 that the term of sustained loads lead to enlarge the creep of RACFST columns. To account for the time-dependent behavior

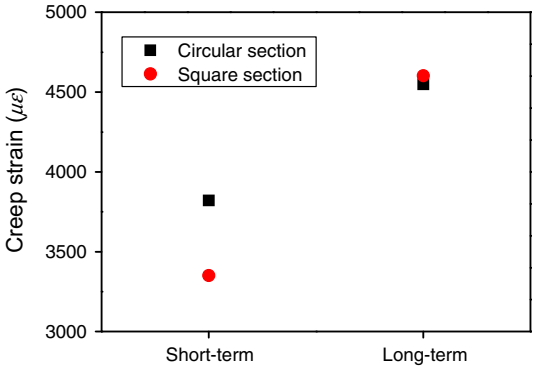


**Fig. 16.** Effect of term of sustained loads on creep of RACFST.

of RACFST columns, Yang [47] proposed formulas for calculating the load carrying capacities of RACFST columns under long-term sustained loads as follows:

$$k_r = \frac{N_u, L}{N_u} \tag{6}$$

$$k_r = k_{cr} \cdot f(n, \lambda) \tag{7}$$

$$f(n,\lambda) = \begin{cases} 1 - 0.07n, & (\lambda \leqslant 40) \\ 0.98 - 0.07n + 0.05\lambda/100 & (\lambda > 40) \end{cases} \tag{8}$$

where $N_{u,L}$ is the load carrying capacity of RACSFT columns under long-term sustained loads; $N_u$ is the load carrying capacity of RACSFT columns under short-term sustained loads, which can be calculated using the theoretical model described by Yang and Han [35]; $k_r$ is the strength index defined to quantify the influence of long-term sustained loads on RACFST columns; $k_{cr}$ is the strength index for conventional CFST columns under long-term sustained loads, and the formulae for $k_{cr}$ can be found in Han et al. [48]; $n$ is the axial load ratio; $\lambda$ is the shear-span ratio of columns.

Geng et al. [49] carried out additional long-term compression tests to establish a proper concrete model to predict the time-dependent response of recycled aggregate concrete in CFST columns. The investigation reported by Geng et al. [49] showed that the total deformations of RACFST columns can increase by up to 50% after 5 months under sustained loading, and the time-dependent deformation of RACFST columns tends to increase linearly with RCA replacement percentage. In addition, it was found that replacing the natural coarse aggregate with the recycled ones also increases the scatter of the time-dependent deformations for the composite members. However, the incorporation of RCA does not affect the rate of creep development of RACFST columns. It should be mentioned that in Geng's tests, the strength of the specimens subjected to sustained loading was slightly higher than the specimens that were not loaded during the long-term test. Geng's findings are similar to those reported by Yang et al. [45]. Geng et al. [49] also introduced amplification factors developed by Fathifazl et al. [50], Brito and Robles [51] to the BS EN 1922 [52] model, and showed the predicted time-dependent deformation of RACFST columns agrees well with test data. The following equations were proposed to describe the ratio of the creep coefficient of RAC ($\varphi_{RAC}$) to that of NAC ($\varphi_{NAC}$):

$$\frac{\varphi_{RAC}}{\varphi_{NAC}} = \left[\frac{1 - (1 - C_{RM}) \times V_{RCA}}{1 - V_A}\right]^{1.33} \tag{9}$$

$$\frac{\varphi_{RAC}}{\varphi_{NAC}} = 3.6548\left(1 - \frac{D_{RA}}{D_{NA}}\right) + 1 \tag{10}$$

$$\frac{\varphi_{RAC}}{\varphi_{NAC}} = 0.0682\left(\frac{W_{RA}}{W_{NA}} - 1\right) + 1 \tag{11}$$

In the above equations, $V_{RCA}$ is the volume (in $m^3$) of recycled coarse aggregates in 1 $m^3$ of concrete, $V_A$ is the volume (in $m^3$) of coarse aggregates in 1 $m^3$ of recycled concrete, $D_{RA}$ and $D_{NA}$ are the bulk specific gravity of recycled and natural coarse aggregates, respectively, and $W_{RA}$ and $W_{NA}$ are the water absorption of the recycled and natural coarse aggregates, respectively.

## 4. Performance of RACFST under cyclic loads

### 4.1. RACFST columns

Experimental work on the performance of recycled aggregate concrete-filled circular steel tube (RACFCST) columns by cyclic loading beam-tests (Fig. 17) was conducted by Yang et al. [53]. In their tests, the composite columns were designed with axial load ratios from 0.05 to 0.52, and three RCA replacement percentages of 0%, 25% and 50% were used to evaluate its influence on the column behavior. Detailed information of the test specimens is given in Table 7. The tests showed that typical failure modes of RACFST columns were similar to those of the corresponding conventional CFST columns, which are global buckling. Fig. 18 shows the load-deformation $P/P_{ue}$–$\Delta$($P$ and $P_{ue}$ are applied lateral midspan load and the experimentally obtained ultimate load, respectively; and $\Delta$ is the midspan displacement corresponding to $P$) and $M/M_{ue}$–$\phi$ ($M$ and $M_{ue}$ are the midspan moment and the experimentally obtained ultimate moment, respectively; and $\phi$ is the midspan curvature corresponding to $M$) curves for an axial load ratio $n$ = 0.25. From Fig. 18, it can be seen that both the load carrying capacities and sectional flexural stiffness of RACFCST columns ($r \neq 0$) are quite comparable to those of the corresponding conventional CFST column ($r$ = 0). Furthermore, RACFST columns also exhibit high ductility levels and energy dissipation capacities.

The cyclic performance of recycled aggregate concrete-filled steel square hollow section beam-columns (often called RACFSST) under a constant axial load and cyclically increasing flexural load was investigated by Yang and Zhu [54]. The loading pattern in these tests is similar to that in the experimental investigation reported by Yang et al. [53]. Detailed information of the test specimens is given in Table 8. The tests were conducted using axial load ratios that varied from 0.05 to 0.52, and for three RCA replacement percentages of 0%, 25% and 50%. Like the cyclic tests performed on RACFCST, the influence of RCA on the failure modes of RACFSST specimens was hardly observed. For all the specimens, buckling

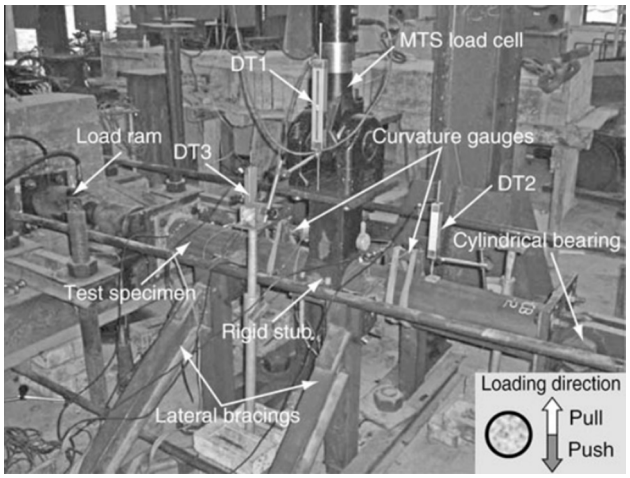


**Fig. 17.** Cyclic beam-test setup (Yang et al. [53]).

**Table 7**
Yang et al's cyclic test specimen details.

| Specimen | Section | $f_{cu}$ (MPa) | $r$ (%) | Tube type | $D$ (or $B$) × $t$ × $L$ (mm) | $f_y$ (MPa) | $n$ [a] | $P_{ue}$ (kN) [a] | SI (%) |
|---|---|---|---|---|---|---|---|---|---|
| L0 | Circular | 60.4 | 0 | Carbon steel | 165 × 2.57 × 1500 | 343.1 | 0.05 | 94.0 | 0 |
| L1 | Circular | 59.2 | 25 | Carbon steel | 165 × 2.57 × 1500 | 343.1 | 0.05 | 92.8 | 1.28 |
| L2 | Circular | 52.2 | 50 | Carbon steel | 165 × 2.57 × 1500 | 343.1 | 0.05 | 92.0 | 2.13 |
| M0 | Circular | 60.4 | 0 | Carbon steel | 165 × 2.57 × 1500 | 343.1 | 0.25 | 106.1 | 0 |
| M1 | Circular | 59.2 | 25 | Carbon steel | 165 × 2.57 × 1500 | 343.1 | 0.25 | 102.9 | 3.06 |
| M2 | Circular | 52.2 | 50 | Carbon steel | 165 × 2.57 × 1500 | 343.1 | 0.25 | 99.3 | 6.46 |
| H0 | Circular | 60.4 | 0 | Carbon steel | 165 × 2.57 × 1500 | 343.1 | 0.48 | 109.0 | 0 |
| H1 | Circular | 59.2 | 25 | Carbon steel | 165 × 2.57 × 1500 | 343.1 | 0.48 | 107.1 | 1.74 |
| H2 | Circular | 52.2 | 50 | Carbon steel | 165 × 2.57 × 1500 | 343.1 | 0.48 | 100.7 | 7.61 |

[a] $n$ is the axial load ratio, $P_{ue}$ is the lateral load of the specimen at failure.

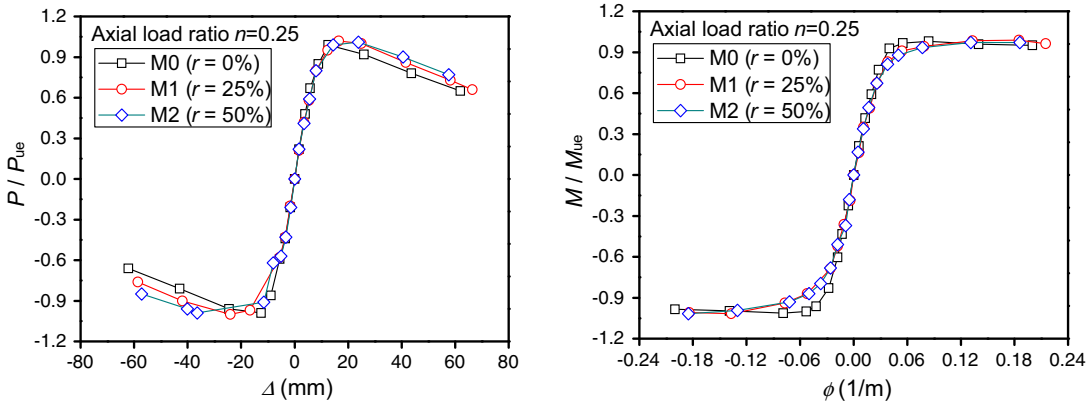


(a) $P/P_{ue}-\Delta$ curves (b) $M/M_{ue}-\phi$ curves

**Fig. 18.** Load-deformation curves of RAC-filled circular steel tube columns (Yang et al. [53]).

**Table 8**
Specimen details in Yang and Zhu's cyclic test.

| Specimen | Section | $f_{cu}$ (MPa) | $r$ (%) | Tube type | $D$ (or $B$) × $t$ × $L$ (mm) | $f_y$ (MPa) | $n$ [a] | $P_{ue}$ (kN) [a] | SI (%) |
|---|---|---|---|---|---|---|---|---|---|
| LA | Square | 60.4 | 0 | Carbon steel | 150 × 2.94 × 1500 | 344.4 | 0.05 | 109.8 | 0 |
| LB-1 | Square | 59.2 | 25 | Carbon steel | 150 × 2.94 × 1500 | 344.4 | 0.05 | 106.9 | 2.64 |
| LB-2 | Square | 59.2 | 25 | Carbon steel | 150 × 2.94 × 1500 | 344.4 | 0.05 | 106.1 | 3.37 |
| LC-1 | Square | 52.2 | 50 | Carbon steel | 150 × 2.94 × 1500 | 344.4 | 0.05 | 105.3 | 4.10 |
| LC-2 | Square | 52.2 | 50 | Carbon steel | 150 × 2.94 × 1500 | 344.4 | 0.05 | 105.4 | 4.01 |
| MA | Square | 60.4 | 0 | Carbon steel | 150 × 2.94 × 1500 | 344.4 | 0.25 | 124.5 | 0 |
| MB-1 | Square | 59.2 | 25 | Carbon steel | 150 × 2.94 × 1500 | 344.4 | 0.25 | 122.8 | 1.37 |
| MB-2 | Square | 59.2 | 25 | Carbon steel | 150 × 2.94 × 1500 | 344.4 | 0.25 | 122.9 | 1.29 |
| MC-1 | Square | 52.2 | 50 | Carbon steel | 150 × 2.94 × 1500 | 344.4 | 0.25 | 119.3 | 4.18 |
| MC-2 | Square | 52.2 | 50 | Carbon steel | 150 × 2.94 × 1500 | 344.4 | 0.25 | 119.1 | 4.34 |
| HA | Square | 60.4 | 0 | Carbon steel | 150 × 2.94 × 1500 | 344.4 | 0.43 | 133.1 | 0 |
| HB-1 | Square | 59.2 | 25 | Carbon steel | 150 × 2.94 × 1500 | 344.4 | 0.43 | 129.8 | 2.48 |
| HB-2 | Square | 59.2 | 25 | Carbon steel | 150 × 2.94 × 1500 | 344.4 | 0.43 | 129.3 | 2.85 |
| HC-1 | Square | 52.2 | 50 | Carbon steel | 150 × 2.94 × 1500 | 344.4 | 0.43 | 127.6 | 4.13 |
| HC-2 | Square | 52.2 | 50 | Carbon steel | 150 × 2.94 × 1500 | 344.4 | 0.43 | 127.2 | 4.43 |

[a] $n$ is the axial load ratio, $P_{ue}$ is the lateral load of the specimen at failure.

of the steel tubes occurred near the rigid stub, and small crack fractures occurred at the corner of the tubes. In addition, as shown in Fig. 19, the RACFSST columns ($r \neq 0$) show comparable load carrying capacities and sectional flexural stiffness as the corresponding conventional CFST column ($r = 0$).

Based on the results exhibited in Yang's studies, the authors considered that CFST columns using recycled aggregate concrete with up to 50% recycled coarse aggregates by weight is suitable for seismic applications.

*4.1.1. Demolished concrete blocks*

It should be noted that the recycled coarse aggregates used in Yang's studies have a conventional sieve grading, i.e., coarse aggregates with sizes 5~16 mm constitute about 55% by weight, and coarse aggregates with sizes 16~26.5 mm constitute about 45%. To simplify the waste concrete recycling process, Wu et al. [55,56] proposed the use of demolished concrete with distinctly larger coarse aggregate sizes. His study includes reinforced concrete beams made from demolished concrete lumps and steel tubular columns made from demolished concrete blocks or lumps. For these composite members, the recycling and reuse of demolished concrete was increased in size from its usual value (i.e., ⩽40 mm) to a higher value (e.g., 50–300 mm for demolished concrete blocks as shown in Fig. 20, and >500 mm in one direction for demolished concrete segments). The use of demolished concrete lumps in reinforced concrete beams can be found in Fig. 21,

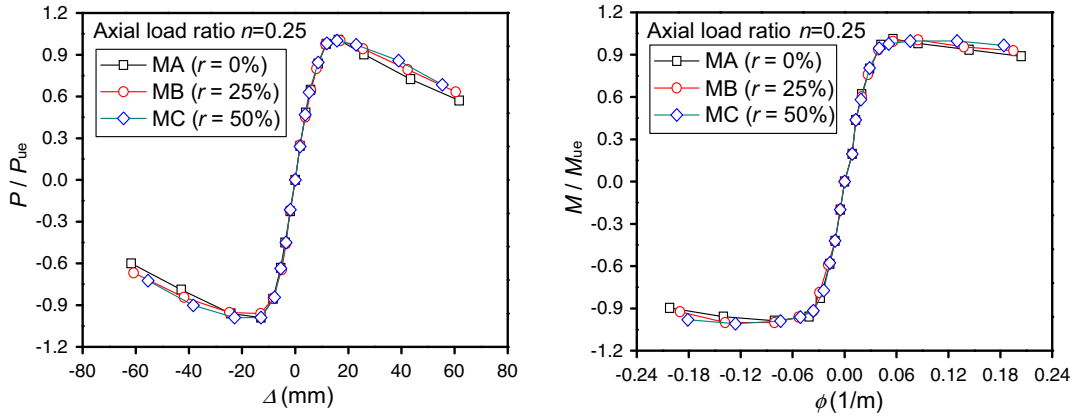


(a) $P/P_{ue}-\Delta$ curves (b) $M/M_{ue}-\phi$ curves

**Fig. 19.** Load-deformation curves of RAC-filled square steel tube columns (Yang and Zhu [54]).

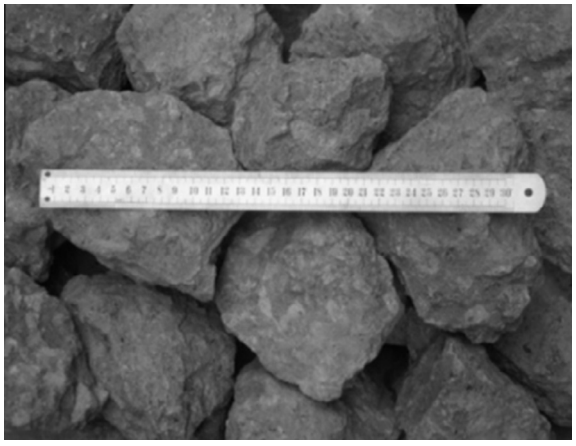

**Fig. 20.** Demolished concrete blocks (Wu et al. [55,56]).

which shows the effect of RCA content on shear loads of hybrid beams. Table 9 lists the comparison of test results and calculated values using existing codes for the full-scale axial loading testes of concrete-filled steel tubular columns incorporating demolished concrete lumps. Hence, it can clearly seen from Fig. 21 and Table 9 that the demolished concrete lumps mixed into concrete lead to decrease the shear capacity of RC beams, while the tested axial load carrying capacity of concrete-filled steel tubular columns incorporating demolished concrete lumps are generally larger than the calculated axial load carrying capacity by using existing codes for concrete-filled steel tubular columns.

In a later study, Wu et al. [64,65] conducted cyclic tests on thin-walled steel tubular columns made from demolished concrete blocks or lumps with fresh concrete to investigate the effects of replacement percentages of the demolished concrete blocks, thickness of the steel tubes, and axial load ratios on the behavior of these composite columns subjected to a constant axial load and cyclic loads (see Fig. 22). Table 10 summarizes the details of the test specimens. Typical load-deformation curves of the test specimens with demolished concrete block replacement percentages of 0%, 25% and 40% are shown in Fig. 23.

Under the same conditions of axial load ratio and thickness of steel tube, it can be seen that the strength of columns made from demolished concrete blocks and fresh concrete is slightly lower than those made from only fresh concrete. With regard to deformations, the ultimate drift ratios of all specimens vary from 2.86% to 5.75%. Thus, the deformation capacities of test columns are larger than the design requirements of interstory drift ratio [66]. In addition, the equivalent viscous damping coefficients of the circular and square specimens were determined to be within the range 0.189 to 0.386 and 0.191 to 0.358, respectively, which indicates that thin-walled steel tubular columns made from demolished concrete blocks and fresh concrete have comparatively good energy dissipation capacity. Therefore, it is expected that these columns when subjected to low to moderate axial load ratios can be used for frame structures in seismic regions.

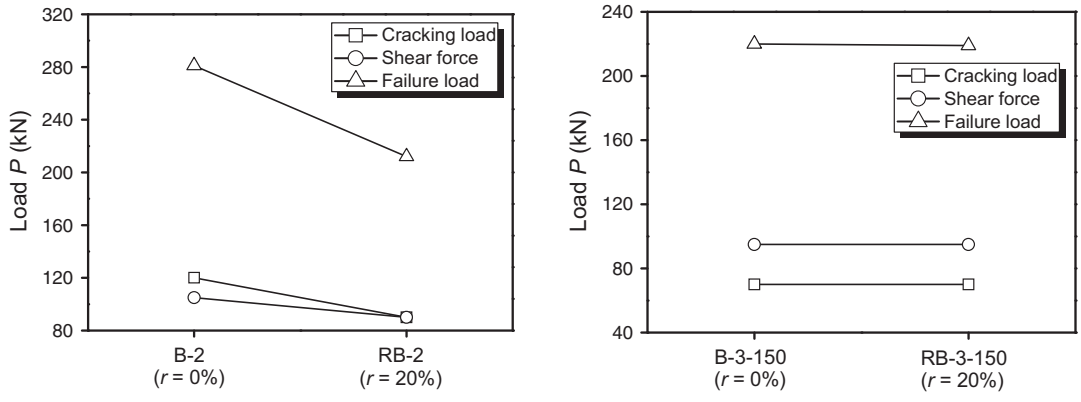


(a) Shear-span ratio = 2.0 (b) Shear-span ratio = 3.0

**Fig. 21.** Effect of RCA content on shear loads of RC beams filled with demolished concrete lumps (Wu et al. [55]).

**Table 9**
The calculated and tested results of full-scale axial loading testes of concrete-filled steel tubular columns incorporating demolished concrete lumps (Wu et al. [56]).

| Code | JCJ [57] | CECS [58] | DL/T [59] | DBJ [60] | ACI [61] | AISC [62] | EC4 [63] |
|---|---|---|---|---|---|---|---|
| $N_{uc}$ (kN) | 14,945 | 15,697 | 13,137 | 12,054 | 10,557 | 11,066 | 14,383 |
| $N_{ue}$ (kN) | | | | 14,500 | | | |
| $N_{ue}/N_{uc}$ | 0.970 | 0.924 | 1.104 | 1.203 | 1.373 | 1.310 | 1.008 |

Note: $N_{uc}$ is the calculated ultimate load carrying capacity; $N_{ue}$ is the experimental ultimate load carrying capacity (mean value of two specimens).

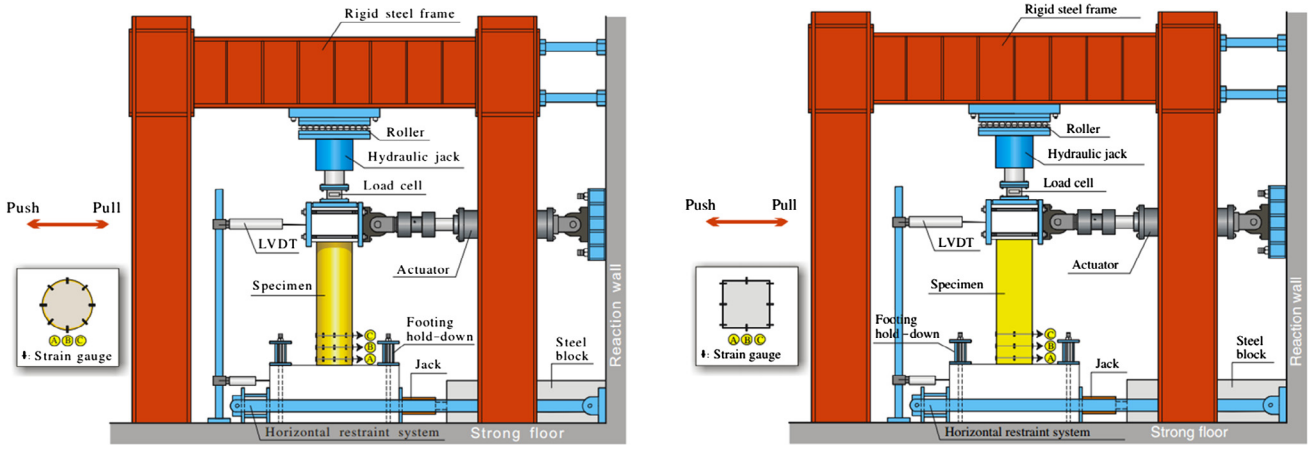


**Fig. 22.** Schematic view of the test setup (Wu et al. [64,65]).

**Table 10**
Cantilever test specimens and test results.

| Specimen | Section | $f_{cu}$ (MPa) | $r$ (%) | Tube type | $D$ (or $B$) × $t$ × $L$ (mm) | $f_y$ (MPa) | $n$ [a] | $P_{ue}$ (kN) [a] | SI (%) |
|---|---|---|---|---|---|---|---|---|---|
| Wu et al. [64] | | | | | | | | | |
| C-T2N2M0 | Circular | 38.2 | 0 | Carbon steel | 300 × 1.78 × 1200 | 255.8 | 0.21 | 72.0 | 0 |
| C-T2N2M2 | Circular | 38.1 | 25 | Carbon steel | 300 × 1.78 × 1200 | 255.8 | 0.21 | 68.9 | 4.31 |
| C-T2N2M4 | Circular | 38.0 | 40 | Carbon steel | 300 × 1.78 × 1200 | 255.8 | 0.21 | 65.2 | 9.44 |
| C-T2N4M0 | Circular | 38.2 | 0 | Carbon steel | 300 × 1.78 × 1200 | 255.8 | 0.42 | 86.1 | 0.00 |
| C-T2N4M2 | Circular | 38.1 | 25 | Carbon steel | 300 × 1.78 × 1200 | 255.8 | 0.42 | 92.6 | -7.55 |
| C-T2N4M4 | Circular | 38.0 | 40 | Carbon steel | 300 × 1.78 × 1200 | 255.8 | 0.42 | 74.2 | 13.82 |
| C-T3N2M0 | Circular | 38.2 | 0 | Carbon steel | 300 × 2.76 × 1200 | 350.0 | 0.21 | 117.8 | 0 |
| C-T3N2M2 | Circular | 38.1 | 25 | Carbon steel | 300 × 2.76 × 1200 | 350.0 | 0.21 | 113.0 | 4.07 |
| C-T3N2M4 | Circular | 38.0 | 40 | Carbon steel | 300 × 2.76 × 1200 | 350.0 | 0.21 | 114.2 | 3.06 |
| C-T3N4M0 | Circular | 38.2 | 0 | Carbon steel | 300 × 2.76 × 1200 | 350.0 | 0.42 | 130.1 | 0.00 |
| C-T3N4M2 | Circular | 38.1 | 25 | Carbon steel | 300 × 2.76 × 1200 | 350.0 | 0.42 | 123.5 | 5.07 |
| C-T3N4M4 | Circular | 38.0 | 40 | Carbon steel | 300 × 2.76 × 1200 | 350.0 | 0.42 | 122.9 | 5.53 |
| C-T6N4M0 | Circular | 38.2 | 0 | Carbon steel | 300 × 5.50 × 1200 | 269.8 | 0.42 | 162.7 | 0 |
| C-T6N4M2 | Circular | 38.1 | 25 | Carbon steel | 300 × 5.50 × 1200 | 269.8 | 0.42 | 161.9 | 0.49 |
| C-T6N4M4 | Circular | 38.0 | 40 | Carbon steel | 300 × 5.50 × 1200 | 269.8 | 0.42 | 160.4 | 1.41 |
| Wu et al. [65] | | | | | | | | | |
| S-T2N2M0 | Square | 48.2 | 0 | Carbon steel | 300 × 1.78 × 1200 | 255.8 | 0.21 | 155.7 | 0 |
| S-T2N2M2 | Square | 45.6 | 25 | Carbon steel | 300 × 1.78 × 1200 | 255.8 | 0.21 | 152.1 | 2.31 |
| S-T2N2M4 | Square | 44.0 | 40 | Carbon steel | 300 × 1.78 × 1200 | 255.8 | 0.21 | 172.9 | −11.05 |
| S-T2N4M0 | Square | 48.2 | 0 | Carbon steel | 300 × 1.78 × 1200 | 255.8 | 0.42 | 193.9 | 0 |
| S-T2N4M2 | Square | 45.6 | 25 | Carbon steel | 300 × 1.78 × 1200 | 255.8 | 0.42 | 188.0 | 3.04 |
| S-T2N4M4 | Square | 44.0 | 40 | Carbon steel | 300 × 1.78 × 1200 | 255.8 | 0.42 | – | – |
| S-T3N2M0 | Square | 48.2 | 0 | Carbon steel | 300 × 2.76 × 1200 | 350.0 | 0.21 | 202.7 | 0 |
| S-T3N2M2 | Square | 45.6 | 25 | Carbon steel | 300 × 2.76 × 1200 | 350.0 | 0.21 | 206.7 | −1.97 |
| S-T3N2M4 | Square | 44.0 | 40 | Carbon steel | 300 × 2.76 × 1200 | 350.0 | 0.21 | 170.4 | 15.93 |
| S-T3N4M0 | Square | 48.2 | 0 | Carbon steel | 300 × 2.76 × 1200 | 350.0 | 0.42 | 261.9 | 0 |
| S-T3N4M2 | Square | 45.6 | 25 | Carbon steel | 300 × 2.76 × 1200 | 350.0 | 0.42 | 241.2 | 7.90 |
| S-T3N4M4 | Square | 44.0 | 40 | Carbon steel | 300 × 2.76 × 1200 | 350.0 | 0.42 | 253.9 | 3.05 |
| S-T6N4M0 | Square | 48.2 | 0 | Carbon steel | 300 × 5.5 × 1200 | 269.8 | 0.42 | 328.0 | 0 |
| S-T6N4M2 | Square | 45.6 | 25 | Carbon steel | 300 × 5.5 × 1200 | 269.8 | 0.42 | 317.9 | 3.08 |
| S-T6N4M4 | Square | 44.0 | 40 | Carbon steel | 300 × 5.5 × 1200 | 269.8 | 0.42 | 305.2 | 6.95 |

[a] $n$ is the axial load ratio, $P_{ue}$ is the lateral load of the specimen at failure.

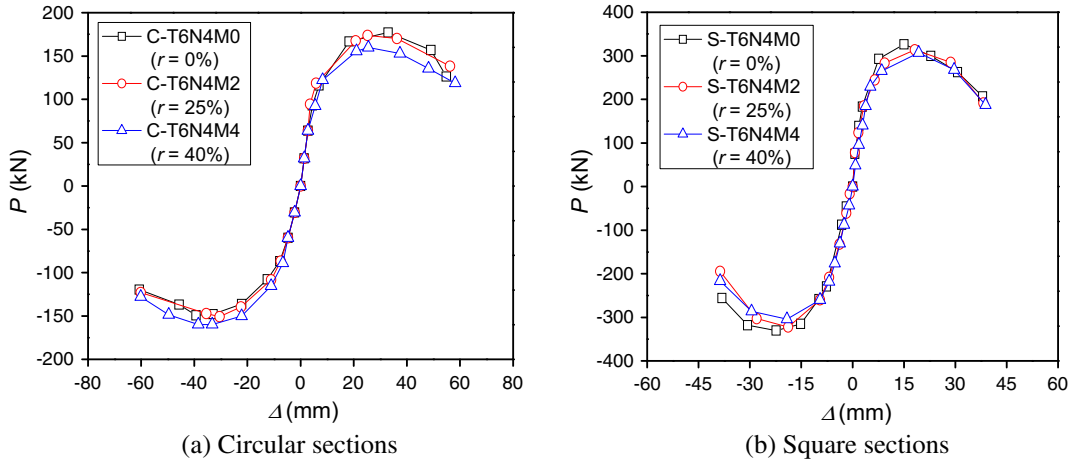


(a) Circular sections (b) Square sections

**Fig. 23.** Typical load-deflection curves of steel tube columns filled with demolished concrete blocks and fresh concrete (Wu et al. [64,65]).

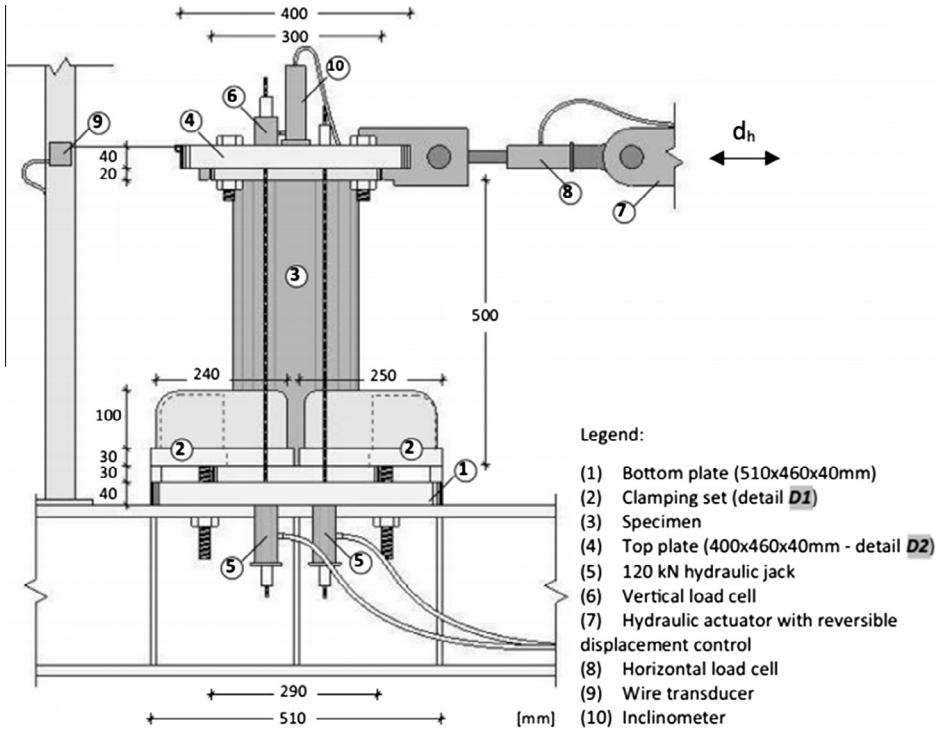


**Fig. 24.** Schematic view of the test setup (Duarte et al. [67]).

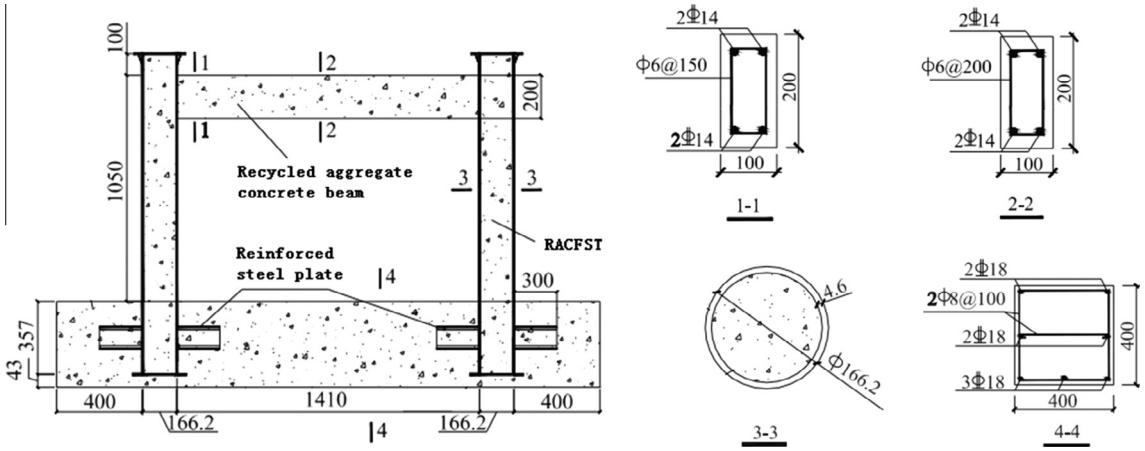


**Fig. 25.** RACFST plane frame: dimensions (Chen et al. [68]).

**Fig. 26.** RACFST plane frame: test setup (Chen et al. [68]).

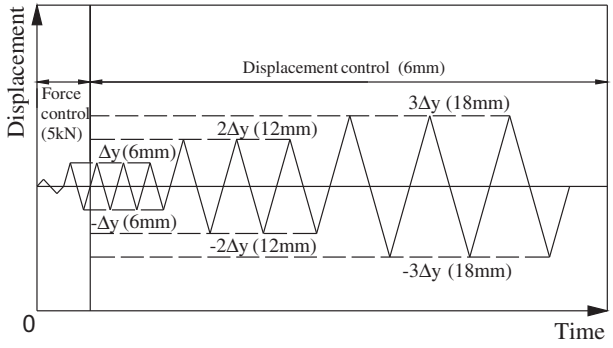


**Fig. 27.** RACFST plane frame: loading history (Chen et al. [68]).

#### 4.1.2. Rubberized concrete

Rubberized concrete is a type of concrete in which natural aggregates are partially replaced with rubber aggregates. These rubber aggregates are recycled from end-of-life tires, and thus it has the potential to reduce environmental impacts related to both the dumping of tires in landfills and the extraction of natural aggregates from quarries. Rubberized concrete is a type of concrete that has been studied for the last three decades and is emerging as a viable construction material for use in structural applications where ductility and energy dissipation are key requirements. Duarte et al. [67] conducted an experimental investigation on the cyclic behavior of short steel tubes filled with rubberized concrete (Fig. 24). A major finding from this study is that the concrete mix with a low replacement ratio (5% – RuC5) of natural aggregates with tire rubber aggregates leads simultaneously to the lowest decrease in the maximum lateral load and the highest increase in the ductility of CFST columns. Thus, this type of member is quite suitable for use in seismic applications when ductility and energy dissipation are both essential design elements.

### 4.2. RACFST plane frame

An experimental investigation on a 1/3 scale plane frame (Fig. 25) constructed using recycled aggregate concrete-filled circular steel tube (RACFCST) columns and reinforced recycled aggregate concrete (RRAC) beam with 100% RCA replacement percentage was carried out by Chen et al. [68]. In this test, both the RCA and NCA sizes are in the range 5∼20 mm, and the compressive cube strength $f_{cu}$(s) of RAC used for the columns and beam are 53.8 MPa and 47.3 MPa, respectively. In addition, the yield tensile strengths $f_y$(s) of the steel tubes, longitudinal reinforcement and stirrup are 416.0 MPa, 420.3 MPa and 399.9 MPa, respectively. The test setup is shown in Fig. 26. The frame was subjected to a constant gravity load of 750 kN and a low-frequency cyclic lateral load as shown in Fig. 27.

The failure mode observed in the test was the typical strong column-weak beam as shown in Fig. 28. In Fig. 29, the hysteretic loops of the RACFCST column – RRAC beam plane frame is shown. The results of the test frame have shown that the deformation ductility coefficient and the ultimate drift ratio are over 3.0 and 2.63%, respectively. These values are higher than those of reinforced concrete frames made from natural coarse aggregates [69,70].

From these experimental investigations, it can be concluded that frame constructed using reinforced recycled aggregate concrete and recycled aggregate concrete filled steel tubes can be expected to behavior well under cyclic loads, and that an increase in RCA content does not necessarily result in a deterioration of frame performance. This means the use of RAC structural members and RAC composite frames in seismic application are justifiable.

## 5. Strength prediction model for RACFST

With the rapid development of steel and concrete composite structures over the past decades, there have been many studies on the theory and computational methods for concrete-filled steel tubular columns [71–74]. These studies affirm the importance of the replacement percentage of recycled coarse aggregates (RCA) on

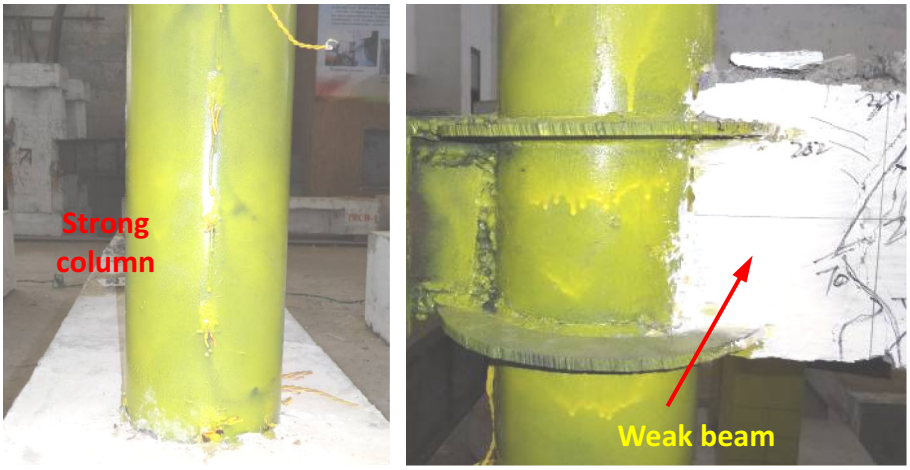


**Fig. 28.** RACFST plane frame: failure pattern (Chen et al. [68]).

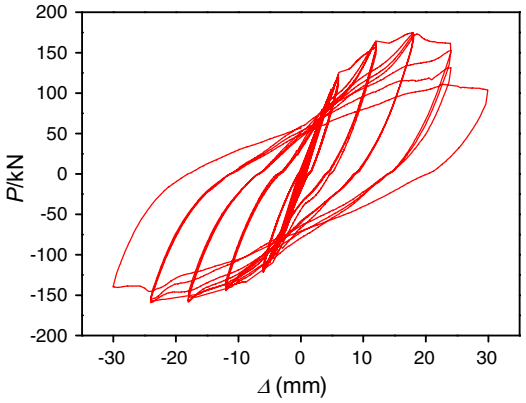


**Fig. 29.** RACFST plane frame: hysteresis loop (Chen et al. [68]).

the compressive and flexural strengths of RACFST members and structures. In general, when the RCA are pre-wetted or pre-soaked, the strength of RACFST decreases with an increase in RCA content. However, the opposite is true when the RCAs are not pre-wetted. As a result, one can apply a reduction or amplification factor to existing design models of concrete-filled steel tubes to estimate the load carrying capacity of RACFST members and structures.

To derive such factors, the experimentally obtained load capacities of RAC-filled square and circular steel tube members and their corresponding conventional concrete-filled steel tube members reported by various researchers were collected, and a strength index (SI) defined as [33]

$$\mathrm{SI} = \frac{N_{e0} - N_{e,r}}{N_{e0}} \tag{12}$$

In the above equation, $N_{e0}$ represents the experimentally obtained load capacities of concrete-filled steel tube members with 0% RCA replacement percentage, and $N_{e,r}$ refers to the experimentally obtained load capacities of concrete-filled steel tube members with $r$% RCA replacement content. The results are plotted in Fig. 30 in which the relationships between the strength index (SI) and RCA replacement percentage ($r$) for RAC-filled square and circular steel tubes are shown.

Using regression analysis, the strength indices (SIs) for the two RACFSTs with different RCA replacement percentages are obtained as:

(1) For RAC-filled square steel tubes

$$\mathrm{SI}_s = \begin{cases} 0.1042\, r & \text{(Pre-wetted RCA)} \\ -0.1043\, r & \text{(No pre-wetting)} \end{cases} \tag{13}$$

(2) For RAC-filled circular steel tubes

$$\mathrm{SI}_c = \begin{cases} 0.0953\, r & \text{(Pre-wetted RCA)} \\ -0.0705\, r & \text{(No pre-wetting)} \end{cases} \tag{14}$$

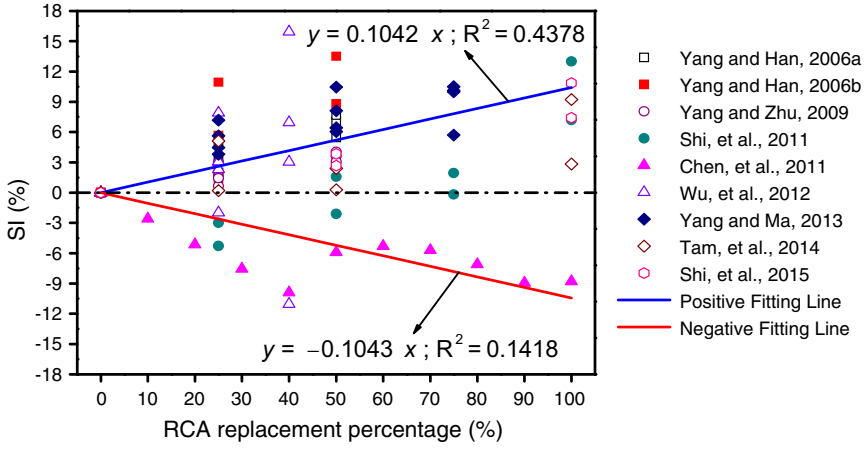


(a) RAC-filled square steel tube members

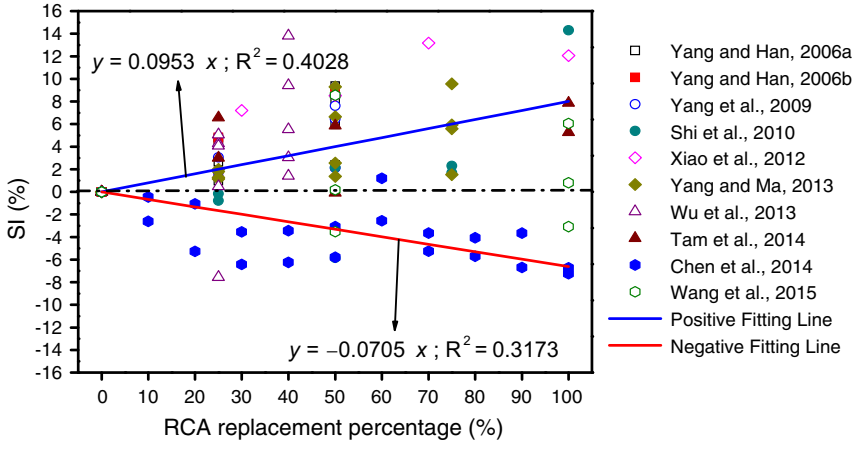


(b) RAC-filled circular steel tube members.

**Fig. 30.** Relationship between SI and RCA replacement percentage.

## 6. Conclusions and recommendations

This paper presents a summary review of relevant research and findings on the bond behavior between recycled aggregate concrete (RAC) and steel tubes, as well as the static and cyclic performance of recycled aggregate concrete-filled steel tubes (RACFST) members and frames. The main conclusions can be summarized as follows:

(1) Bond behavior:
   (a) The bond strength between RAC and steel tube in general increases with an increase in recycled concrete aggregates (RCA) replacement percentage, provided that the RCA used are not pre-soaked.
   (b) The bond strength between RAC and circular steel tubes is almost twice as high as that between RAC and square steel tubes, indicating that the confinement effect of circular steel tubes is superior to that of square steel tubes.

(2) Performance under static loads:
   (c) When compared with CFST beams made from conventional concrete, the initial section flexural stiffness, serviceability-level section flexural stiffness and ultimate bending moment of CFST beams made from RAC are somewhat lower.
   (d) Test on stub columns have shown that on the material level, both strength and deformation of RAC improve due to the confinement of the concrete and strength contribution by the steel tubes; and on the structural level, the ultimate strength of RAC decreases while the corresponding strain increases when the replacement content of RCA is increased.
   (e) When all other parameters are equal, the mechanical properties of RAC confined by steel tubes have been shown to be better than those confined by GFRP tubes.
   (f) The influence of recycled aggregates on the strength and ductility of geopolymeric recycled concrete-filled steel tube columns is generally more noticeable than those of RACFST columns.
   (g) Recycled coarse aggregates without undergoing the pre-wetting process has been shown to enhance the strength and reduce the deformation of RACFST stub columns due to the reduction of effective water-cement ratio in concrete.
   (h) When compared to conventional concrete-filled steel tube columns, the shrinkage and creep strains of RACFST columns are higher, and the long-term load carrying capacity of RACFST columns tends to decrease with an increase in RCA content.

(3) Performance under cyclic loads:
   (i) The cyclic behavior of RACFST members is quite comparable to those made from natural coarse aggregates.
   (j) Tests carried out on RACFST frames have shown that they perform well under cyclic loads. An increase in RCA content does not appear to have a noticeable effect on their performance.

(4) Prediction model:
   Because the strength of RACFST is dependent on whether or not the recycled coarse aggregates used have been pre-wetted, a reduction or amplification factor can be applied to the existing design strengths of concrete-filled steel tubes to predict the load carrying capacities of RACFST members and frames. Based on experimental data reported for members subjected to static and cyclic loads and using regression analysis, simple equations for these factors are proposed.

(5) Recommendations for future studies:
   (k) Because fire can occur over the design life of a structure, study on the mechanical properties of RACFST members exposed to fire should be performed.
   (l) Almost all studies that have been carried out to date and reported herein are focused on member behavior, seismic behavior of substructures composed of RACFST column to beam joints should be investigated thoroughly and design methods for RACFST joints need to be formulated.

## Acknowledgments

The research reported in this paper was supported by the National Natural Science Foundation of China (No. 51578163), the Study Abroad Program for Excellent Ph.D. Students of Guangxi Zhuang Autonomous Region and the Innovation Project of Guangxi Graduate Education (No. YCBZ2014007).

## References

[1] Eurostat, Waste Statistics in Europe. Available at: <epp.eurostat.ec.europa.eu>, 2015 (last accessed in 09.03.15).
[2] Xiao Jianzhuang, Li Jiabin, Ch Zhang, Mechanical properties of recycled aggregate concrete under uniaxial loading, Cem. Concr. Res. 35 (6) (2005) 1187–1194.
[3] Liu Qiong, Xiao Jianzhuang, Sun Zhihui, Experimental study on the failure mechanism of recycled concrete, Cem. Concr. Res. 41 (10) (2011) 1050–1057.
[4] D. Matias, J. de Brito, A. Rosa, D. Pedro, Mechanical properties of concrete produced with recycled coarse aggregates – influence of the use of superplasticizers, Constr. Build. Mater. 44 (2013) 101–109.
[5] F. Ceia, J. Raposo, M. Guerra, E. Júlio, J. de Brito, Shear strength of recycled aggregate concrete to natural aggregate concrete interfaces, Constr. Build. Mater. 109 (2016) 139–145.
[6] Lye Chaoqun, K. Dhir Ravindra, S. Ghataora Gurmel, Li Hui, Creep strain of recycled aggregate concrete, Constr. Build. Mater. 102 (2016) 244–259.
[7] S.C. Kou, C.S. Poon, Enhancing the durability properties of concrete prepared with coarse recycled aggregate, Constr. Build. Mater. 35 (2012) 69–76.
[8] C. Thomas, J. Setién, J.A. Polanco, P. Alaejos, M. Sánchez de Juan, Durability of recycled aggregate concrete, Constr. Build. Mater. 40 (2013) 1054–1065.
[9] T. Vieira, A. Alves, J. Brito, J.R. de Correia, R.V. Silva, Durability-related performance of concrete containing fine recycled aggregates from crushed bricks and sanitary ware, Mater. Des. 90 (2016) 767–776.
[10] Saatcioglu Murat, R. Razvi Salim, Strength and ductility of confined concrete, ASCE J. Struct. Eng. 118 (6) (1992) 1590–1607.
[11] Xiao Yan, He Wenhui, Choi Kang Kyu, Confined concrete-filled tubular columns, ASCE J. Struct. Eng. 131 (3) (2005) 488–497.
[12] K. Konno, Y. Sato, Y. Kakuta, M. Ohira, The property of recycled concrete column encased by steel tube subjected to axial compression, Trans. Jpn. Concr. Inst. 19 (2) (1997) 231–238.
[13] P.J. Nixon, Recycled concrete as an aggregate for concrete-a review, Mater. Struct. 11 (5) (1978) 371–378.
[14] J.M. Sánchez de, G.P. Alaejos, Study on the influence of attached mortar content on the properties of recycled concrete aggregate, Constr. Build. Mater. 23 (2) (2009) 872–877.
[15] Z.P. Chen, J.J. Xu, H.H. Zheng, Y.S. Su, J.Y. Xue, J.T. Li, Basic mechanical properties test and stress-strain constitutive relations of recycled coarse aggregate concrete, J. Build. Mater. 16 (1) (2013) 24–32 (in Chinese).
[16] Xiao Jianzhuang, Li Long, Shen Luming, Poon Chi Sun, Compressive behaviour of recycled aggregate concrete under impact loading, Cem. Concr. Res. 71 (2015) 46–55.
[17] Paula Folino, Hernán Xargay, Recycled aggregate concrete – mechanical behavior under uniaxial and triaxial compression, Constr. Build. Mater. 56 (2014) 21–31.
[18] Hou Yueqin, Su Ji Xiaoping, Zhang Wengang Xiuli, Liu Lingqin, Laboratory investigations of activated recycled concrete aggregate for asphalt treated base, Constr. Build. Mater. 65 (2014) 535–542.
[19] Z.P. Chen, J.J. Xu, Y. Liang, Y.S. Su, Bond behaviors of shape steel embedded in recycled aggregate concrete and recycled aggregate concrete filled in steel tubes, Steel Compos. Struct. 17 (6) (2014) 929–949.
[20] L. Butler, J.S. West, S.L. Tighe, The effect of recycled concrete aggregate properties on the bond strength between RCA concrete and steel reinforcement, Cem. Concr. Res. 41 (10) (2011) 1037–1049.
[21] Tao Zhong, Han Linhai, Brian Uy, Chen Xian, Post-fire bond between the steel tube and concrete in concrete-filled steel tubular columns, J. Constr. Steel Res. 67 (3) (2011) 484–496.

[22] Yang Youfu, Han Linhai, Compressive and flexural behavior of recycled aggregate concrete filled steel tubes (RACFST) under short-term loadings, Steel Compos. Struct. 6 (3) (2006) 257–284.
[23] Yang Youfu, Ma Guoliang, Experimental behavior of recycled aggregate concrete filled stainless steel tube stub columns and beams, Thin Walled Struct. 66 (2013) 62–75.
[24] X.S. Shi, Q.Y. Wang, X.L. Zhao, F. Collins, Strength and ductility of recycled aggregate concrete filled composite tubular stub columns, in: 21st Australasian Conference on the Mechanics of Structures and Materials, Melbourne, Australia, 2010, pp. 83–89.
[25] Xiao Jianzhuang, Huang Yijie, Yang Jie, Ch Zhang, Mechanical properties of confined recycled aggregate concrete under axial compression, Constr. Build. Mater. 26 (2012) 591–603.
[26] Wang Yuyin, Chen Jie, Geng Yue, Testing and analysis of axially loaded conventional-strength recycled aggregate concrete filled steel tubular stub columns, Eng. Struct. 86 (2015) 192–212.
[27] Vivian W.Y. Tam, Zhibin Wang, Tao Zhong, Behavior of recycled aggregate concrete filled stainless steel stub columns, Mater. Struct. 47 (1) (2014) 293–310.
[28] B. Uy, Z. Tao, L.H. Han, Behavior of short and slender concrete-filled stainless steel tubular columns, J. Constr. Steel Res. 67 (3) (2011) 360–378.
[29] X. Dai, D. Lam, Axial compressive behavior of stub concrete-filled columns with elliptical stainless steel hollow sections, Steel Compos. Struct. 10 (6) (2010) 517–539.
[30] J.F. Dong, Q.Y. Wang, Z.W. Guan, Structural behavior of recycled aggregate concrete filled steel tube columns strengthened by CFRP, Eng. Struct. 48 (2013) 532–542.
[31] Huang Yijie, Xiao Jianzhuang, Ch Zhang, Theoretical study on mechanical behavior of steel confined recycled aggregate concrete, J. Constr. Steel Res. 76 (2012) 100–111.
[32] Liu Yixiang, Zha Xiaoxiong, Gong Guobin, Study on recycled-concrete-filled steel tube and recycled concrete based on damage mechanics, J. Constr. Steel Res. 71 (2012) 143–148.
[33] Shi Xiaoshuang, Wang Qingyuan, Zhao Xiaoling, G. Collins Frank, Structural behavior of geopolymeric recycled concrete filled steel tubular columns under axial loading, Constr. Build. Mater. 81 (2015) 187–197.
[34] Z.P. Chen, J.J. Xu, J.Y. Xue, Y.S. Su, Performance and calculations of recycled aggregate concrete-filled steel tubular (RACFST) short columns under axial compression, Int. J. Steel Struct. 14 (1) (2014) 31–42.
[35] Yang Youfu, Han Linhai, Experimental behavior of recycled aggregate concrete filled steel tubular columns, J. Constr. Steel Res. 62 (12) (2006) 1310–1324.
[36] Eurocode 4, Design of Composite Steel and Concrete Structures, Part1.1: General Rules and Rules for Buildings (Together With United Kingdom National Application Document). DD ENV 1994-1-1:1994, British Standards Institution, London W1A2BS, 1994.
[37] ACI 318-99, Building Code Requirements for Structural Concrete and Commentary, American Concrete Institute, Detroit, Farmington Hills (MI, USA), 1999.
[38] AIJ, Recommendations for Design and Construction of Concrete Filled Steel Tubular Structures, Architectural Institute of Japan, Tokyo (Japan), 1997.
[39] AISC-LRFD, Load and Resistance Factor Design Specification for Structural Steel Buildings, second ed., American Institute of Steel Construction (AISC), Chicago (USA), 1999.
[40] British Standard Institute, BS5400, Part 5. Concrete and Composite Bridges, 1979. London (UK).
[41] DBJ 13-51-2003, Technical Specification for Concrete-Filled Steel Tubular Structures, 2003. Fuzhou (in Chinese).
[42] R.V. Silva, J. Brito, R.K. De Dhir, Prediction of the shrinkage behavior of recycled aggregate concrete: a review, Constr. Build. Mater. 77 (2015) 327–339.
[43] W.Y. Tam Vivian, Kotrayothar Duangthidar, Xiao Jianzhuang, Long-term deformation behavior of recycled aggregate concrete, Constr. Build. Mater. 100 (2015) 262–272.
[44] Lye Chaoqun, K. Dhir Ravindra, S. Ghataora Gurmel, Li Hui, Creep strain of recycled aggregate concrete, Constr. Build. Mater. 102 (2016) 244–259.
[45] Yang Youfu, Han Linhai, Wu Xin, Concrete shrinkage and creep in recycled aggregate concrete-filled steel tubes, Adv. Struct. Eng. 11 (4) (2008) 383–396.
[46] ACI Committee 209, Prediction of Creep, Shrinkage and Temperature Effects in Concrete Structures, American Concrete Institute, Detroit, MI, USA, 1992.
[47] Yang Youfu, Behavior of Recycled Aggregate Concrete-Filled Steel Tubular Columns Under Long-Term Sustained Loads, Adv. Struct. Eng. 14 (2) (2011) 189–206.
[48] L.H. Han, Z. Tao, W. Liu, Effects of sustained load on concrete-filled hollow structural steel columns, ASCE J. Struct. Eng. 130 (9) (2004) 1392–1404.
[49] Geng Yue, Wang Yuyin, Chen Jie, Time-dependent behavior of recycled aggregate concrete-filled steel tubular columns, ASCE J. Struct. Eng. 141 (10) (2015) 11–12.
[50] G. Fathifazl, A.G. Ghani Razaqpur, O.B. Isgor, A. Abbas, B. Fournier, S. Foo, Creep and drying shrinkage characteristics of concrete produced with coarse recycled concrete aggregate, Cement Concr. Compos. 33 (10) (2011) 1026–1037.
[51] J. Brito, R. Robles, Recycled aggregate concrete (RAC) methodology for estimating its long-term properties, Indian J. Eng. Mater. Sci. 17 (6) (2010) 449–462.
[52] BSI (British Standards Institution), Eurocode 2: Design of Concrete Structures-Part 1-1: General Rules and Rules for Buildings. BS EN 1992, 2004. London.
[53] Yang Youfu, Han Linhai, Zhu Lintao, Experimental performance of recycled aggregate concrete-filled circular steel tubular columns subjected to cyclic flexural loadings, Adv. Struct. Eng. 12 (2) (2009) 183–194.
[54] Yang Youfu, Zhu Lintao, Recycled aggregate concrete filled steel SHS beam-columns subjected to cyclic loading, Steel Compos. Struct. 9 (1) (2009) 19–38.
[55] B. Wu, Z. Xu, Z.J. Ma, Q.X. Liu, W. Liu, Behavior of reinforced concrete beams filled with demolished concrete lumps, Struct. Eng. Mech. 40 (3) (2011) 411–429.
[56] B. Wu, X.Y. Zhao, Q.X. Liu, J.S. Zhang, Full-scale axial loading tests of concrete-filled steel tubular columns incorporating demolished concrete lumps, in: Proceedings of the Second International Conference on Waste Engineering and Management, 2010, pp. 36–45.
[57] Chinese Standard JCJ 01-89, Specification for Design and Construction of Concrete-Filled Steel Tubular Structures, Tingji University Press, Shanghai, 1989.
[58] Chinese Standard CECS 28: 90, Specification for Design and Construction of Concrete-Filled Steel Tubular Structures, China Plan Press, Beijing, 1990.
[59] Chinese Standard DL/T 5085-1999, Code for Design of Steel-Concrete Composite Structure, China Electric Power Press, Beijing, 1999.
[60] Chinese Standard DBJ 13-51-2003, Specification for Concrete-Filled Steel Tubular Structures, Construction Department of Fujian Province, Fuzhou, 2003.
[61] ACI Committee 318 (ACI 318-08), Building Code Requirements for Structural Concrete and Commentary, American Concrete Institute, Detroit, 2008.
[62] ANSI/AISC 360-05, Specification for Structural Steel Buildings, American Institute of Steel Construction, Chicago, 2005.
[63] EN 1994-1-1: 2004 (EC 4), Design of Steel and Concrete Structures. Part 1: General Rules and Rules for Building, European Committee for Standardization, Brussels, 2004.
[64] Wu Bo, Zhao Xinyu, Zhang Jinsuo, Yang Yong, Cyclic testing of thin-walled circular steel tubular columns filled with demolished concrete blocks and fresh concrete, Thin Walled Struct. 66 (2013) 50–61.
[65] Wu Bo, Zhao Xinyu, Zhang Jinsuo, Cyclic behavior of thin-walled square steel tubular columns filled with demolished concrete lumps and fresh concrete, J. Constr. Steel Res. 77 (2012) 69–81.
[66] Chinese Standard GB 50011-2010, Code for Seismic Design of Buildings, China Architecture and Building Press, Beijing, 2010.
[67] A.P.C. Duarte, B.A. Silva, J. Brito, E. de Júlio, J.M. Castro, Experimental study on short rubberized concrete-filled steel tubes under cyclic loading, Compos. Struct. 136 (2016) 394–404.
[68] Chen Zongping, Zhang Xianggang, Xue Jianyang, Su Yisheng, Experimental study on seismic performance of recycled aggregate concrete filled steel tube column and reinforced recycled aggregate concrete beam frame, China Civil Eng. J. 47 (10) (2014) 22–31 (in Chinese).
[69] ASCE, Minimum Design Loads for Buildings and Other Structures. ASCE7-05, 2005.
[70] Aidcer L. Vidot-Vega, Mervyn J. Kowalsky, Drift, strain limits and ductility demands for RC moment frames designed with displacement-based and force-based design methods, Eng. Struct. 51 (2013) 128–140.
[71] L.H. Han, Concrete-Filled Steel Tubular Structures-Theory and Practise, China Science Press, Peking, 2007.
[72] C.S. Cai, Modern Steel and Concrete Composite Structure, People's Communication Press, Peking, 2007.
[73] S.T. Zhong, Unified Theory of Concrete Filled Steel Tube – Research and Application, Tsinghua University Press, Peking, 2006.
[74] F.X. Ding, Z.W. Yu, Y. Bai, Y.Z. Gong, Elasto-plastic analysis of circular concrete-filled steel tube stub columns, J. Constr. Steel Res. 67 (10) (2011) 1567–1577.